ANALYSIS OF BONE CUTTING MECHANICS IN ORTHOPEDIC SURGERY

By

ARJUN DHAMODHARAN

Bachelor of Technology in Mechanical Engineering

Amrita School of Engineering

Coimbatore, India

2012

Submitted to the Faculty of the
Graduate College of the
Oklahoma State University
in partial fulfillment of
the requirements for
the Degree of
MASTER OF SCIENCE
July, 2016

ANALYSIS OF BONE CUTTING MECHANICS IN

ORTHOPEDIC SURGERY

Thesis Approved:

Dr. Xiaoliang Jin

Thesis Adviser

Dr. Daniel J Burba

Dr. Raman Singh

ACKNOWLEDGEMENTS

I would like to express my sincere gratitude and appreciation to my supervisor Dr.Xiaoliang Jin for his invaluable inspiration and motivation throughout my research. Dr.Jin has always been a great mentor and has inspired me through enthusiasm and welcoming nature. I truly appreciate his advice, encouragement and support without which this thesis would not have been possible.

I would like thank Dr. Daniel Burba and Dr. Raman Singh for serving in my thesis committee and providing valuable suggestions for improvement. I would like to thank Dr. Jenna Young for her valuable time and help with sample preparation, and advice on preservation techniques.

I would like to thank Exakt Technologies in Oklahoma City for lending us their pathological saw for cutting cannon bones to make specimens.

I am truly indebted to my parents for their unconditional love and support throughout my studies. I would like to thank my brother for his valuable advice.

I greatly value my colleagues Anju, Boyuan, Gopal, Naresh and Vinay in Precision Manufacturing Processes Lab for their friendship and help during my research. I would like to thank all my friends for being a valuable part of my journey until this point.

Name: ARJUN DHAMODHARAN

Date of Degree: 15TH JULY, 2016

Title of Study: MASTER OF SCIENCE

Major Field: MECHANICAL AND AEROSPACE ENGINEERING

Abstract:

Bone cutting has been widely used in orthopedic surgery for repairing bone fractures and attaching implantable prosthetics. Temperature rise in the cutting process can cause necrosis when it is beyond a threshold value, depending on the species and age of the bone. Excessive cutting force may induce bone micro-fractures which lead to breakdown at the repair site. This thesis investigates the effect of cutting parameters on temperature and force in cutting of bovine and equine cannon bones. Vibration assisted drilling which enables intermittent contact between the cutting tool and the bone is conducted, and the effect of vibration assistance on the cutting performance is evaluated. Damages caused at the drill site of the bone are characterized by Micro-CT. Bone milling is used to shave the end of the bone to fit the plane of the artificial joint precisely. In this study, Taguchi method is used to evaluate the influence of the parameters such as spindle speed, feed rate and depth of cut on the milling process. This thesis provides insights in the mechanics of bone cutting process used in orthopedic surgery. The results provide optimum cutting operations to minimize the process induced bone damage.

TABLE OF CONTENTS

CHAPTER PAGE

LIST OF TABLES

Table Page

LIST OF FIGURES

Figure Page

CHAPTER 1

INTRODUCTION

1.1 Background

Bone fracture is a common injury to human and animal bodies due to accident, disease or aging. Fractures are usually caused by sudden occurrence of external load that exceeds bone strength, or cyclic loads (well below bone strength) that gradually accumulate bone damages at a rate that cannot be repaired. When a bone is broken, the periosteum (outer surface cell layer) and endosteum (inner surface cell layer next to the marrow) provide bone-forming cells which aid in bridging the fracture. Drilling is usually performed for screw insertion and plate fixing operation in order to restore function, length and aid in healing of bone. The bone cutting is one of the oldest surgical procedures in the history of medicine. At present, implant surgeries on knee and hip are considered the most common practices which are performed all around the world. For example, the number of hip fractures world-wide was estimated to be 1.66 million in 1990 and expected to increase to 6.26 million by 2050 [1]. A well-known treatment in bone surgery is joint replacement by implanting mechanical structures made of metal and composites to imitate kinematic and dynamic functions of a human joint. Approximately, around 300,000 knee arthroplasties are performed each year in the United States alone, with the total number increasing annually [2]. Originally, screws used for orthopedic surgery are made of bio-compatible metals, such as titanium, stainless steel and cobalt chrome alloys. In recent years,

direct machining of bone for producing bone screws to replace metals is becoming popular. Bone screws has the advantages of enabling micro movements at fracture sites and minimizing per-implant osteopenia (a condition where bone's mineral density is lower than normal) [3] Bone cutting operations include scraping, grooving, sawing, drilling, milling, boring, grafting and shearing. Among these methods, drilling is a surgical operation that is most discussed in the literature. Figure 1.1 shows an example of study of fixation pin insertion after stepwise drilling of bones[4] .

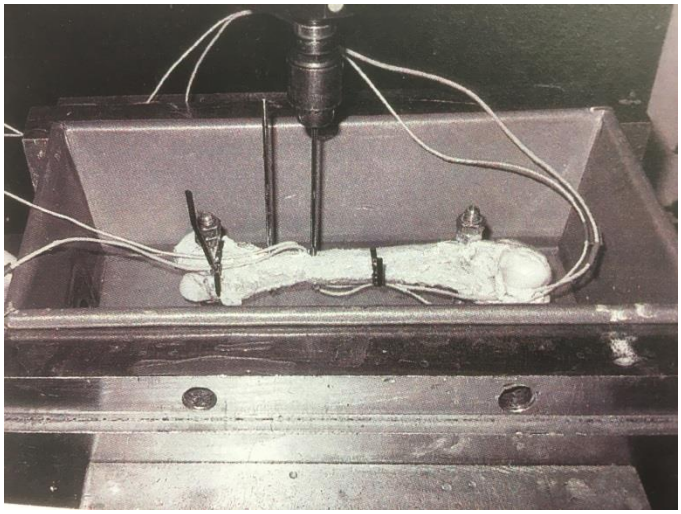

Fig. 1.1. Image of testing procedure for insertion of fixation pin [4]

Characterization of bone machining process and machined bone quality is critical for surgeons to achieve optimum operation conditions. Bone machining has been a challenge because of the sensitivity of osteocytes to the heat produced during the machining process. The heat causes thermal damages on bone cells and can result in necrosis. It can also lead to cutting problems like clogging or built up edge. If the cutting parameters such as feed speed, spindle speed are not selected properly, the cutting force induces further bone cracks, which lead to the loosening of fixation. Therefore, determination of temperature and force is necessary to avoid the damage to the bone.

Bone is one of the fastest healing tissues in the body compared to tendons and ligaments. For example, humans and small animals heal faster when compared to equine. With the correct treatment, horses can return to their previous athletic activity. Internal fixation is a technique that makes fracture repair possible and allowing weight-bearing on a fractured leg. This technique requires machining like drilling and tapping to be performed on the bone. Drilling of bone is a frequently used process for orthopedic implantation by equine surgeons.

Bone material plays a significant role in the force and temperature generation in bone machining process. New machining techniques have been developed for bone cutting in orthopedic surgery in recent years. Vibration assisted drilling is a cutting process where the tool vibrates at a certain frequency in the z axis, resulting in intermittent or discontinuous cutting process. The bone-tool interaction in conventional drilling and ultrasonic vibration assisted drilling has been of interest to researchers [5]. The ultrasonic vibration assisted cutting has already been implemented in aerospace industries to cut metal alloys and composites. It has been confirmed that the reduced temperature and cutting forces are achieved with vibration assistance. Hence, the curiosity lies in the behavior of biomaterial under the influence of ultrasonic vibration. The literature available so far has been concentrating on bovine femur bones, and no research has been done on the equine cannon bone, which is prone to fracture more often than the bovine bone. The high density of the equine bone may also make it susceptible to thermal injury and micro-fracture during cutting. Bovine cannon bones are used instead of equine, as the samples are more available and expendable when compared to equine bone.

As previously mentioned, arthroplasty is a surgical replacement of joints with artificial parts. The cut ends of the bones must be milled to properly accept the implant. Therefore, it is necessary to obtain the optimum milling parameters to conduct the procedure. The milling operation is also conducted to prepare specimens to perform studies related to temperature measurement on bones, while using thermocouples. Drilling of equine cannon bone is the heart of this thesis, and there is

no research material available on cannon bone milling. Hence, this topic is also addressed as part of this thesis.

There are two parts in this research. Firstly, In vitro experimental investigations are conducted to analyze the effect of process parameters on cortical temperature and the drilling forces in equine cannon bone drilling. Particular attention has been paid to benefits, if any, of vibration assisted drilling. The damage caused by the drilling processes are evaluated by micro-CT. Micro-CT of the drilled bones can provide the detailed information on the effect of damage caused by each cutting condition and the comparison of the cracks from results can provide the reasoning behind the caused damage. The investigator is unaware of any research that has been conducted on verifying the effects of vibration assisted drilling on equine bone. Hence, one of the objectives of the research is to investigate the effects of two drilling techniques- conventional versus vibration assisted.

Secondly, statistical analysis is performed on experimental data gathered during milling of bovine cannon bone to find optimum milling parameters such as spindle speed, feed per tooth and depth of cut.

1.2 Specific Aims and Objectives

The main objective of this research is to gain an in depth understanding of drilling of equine cannon bone in vitro with conventional and vibration assisted drilling process, and determine the optimum cutting parameters in order to improve the surgical procedure. It is expected that the results of this research will be used as a benchmark to incorporate the use of vibration assisted drilling in orthopedic surgery for equine bone.

The experiments carried out in this research are mainly focused on simulating the conditions encountered during cutting of cortical bone in orthopedic surgery in a machining center and study

the influence of various cutting parameters on temperature and cutting forces in the presence and absence of vibration.

The specific aims of this thesis are:

1. To study the influence of cutting parameters on bone temperature and cutting forces of equine and bovine metacarpal and metatarsal bone in vitro.

2. To investigate the damage caused by drilling in both conventional and vibration assisted drilling on equine metacarpal and metatarsal bone in vitro using micro-CT.

3. To measure cutting temperatures experimentally using thermocouples in the in vitro study of bovine and equine metacarpal bone.

1.3 Organization of thesis

A brief overview of the various chapters is as follows.

Chapter 2: Literature Review

A review of the literature work in bone machining is presented in this chapter. Bone preservation techniques are discussed. A brief discussion of various bone machining processes like bone milling and bone drilling is described. Various new bone drilling techniques and vibration assisted machining techniques has been outlined.

Chapter 3: Conventional and Vibration Assisted Drilling of Equine Cannon Bone.

A detailed description of sample preparation, experimental setup of both conventional and vibration assisted drilling, and experimental procedure is given in this chapter. Results and analysis of conventional versus vibration assisted drilling of equine cannon bone is discussed.

Chapter 4: Milling of Bovine Cannon Bone

The experimental setup, procedure and results are discussed in detail. Statistical analysis is performed using Taguchi method to find the most influencing cutting parameter for each response (temperature, surface roughness and cutting forces). Response Optimizer tool is used to find the most optimized cutting condition for a desired response.

Chapter 5: Conclusion and Future scope

This chapter documents the work discussed in this thesis with concluding remarks and areas for future scope.

CHAPTER 2

LITERATURE REVIEW

In this chapter, previous studies in bone preservation techniques, temperature and force measurement techniques in bone machining are reviewed. The research related to vibration assisted machining for bones is also discussed. The knowledge gap based on the literature survey and the motivation of this study are introduced.

2.1 Equine Metacarpal and Metatarsal Bone Anatomy and Biomechanical Properties

Cannon bone is a weight bearing bone in the lower leg and stretches from the knee joint to the ankle (fetlock joint). In medical terminology, it refers to the third metacarpal or metatarsal bone in hoof stock animals. This third metacarpal bone of thoroughbred racehorses is an excellent example of the ability of skeleton to adapt to variable physical activity. This adapting mechanism is also called as Wolff's law [6].

The bone is a complex tissue with multiple functions. But, its primary function is to be stiff, resisting deformation. Bone strength can be increased in a number of ways, e.g., by adding bone mass, changing geometry of bone or by microstructure alterations via processes such as Haversian remodeling. The strength of the bone is adapted with respect to the forces undergone by a bone. Typically bones are loaded in four possible ways- Axial compression, Bending, Twisting and Shear [6]. But cannon bone is mostly loaded with compression force, as it is the weight bearing bone .The cannon bone is a cortical bone, and its osteons are called Haversian

systems [7]. They are cylindrical in shape and form branching network within cortical bone. The osteons of cannon bone are as shown in the figure 2.1.

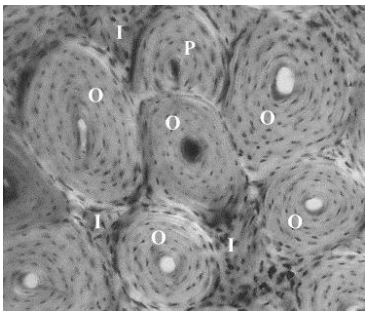

Fig. 2.1. Typical osteonal structure in the equine third metacarpal [8].

The dorsal cortex of the third metacarpal bone is one of the most common injuries that results in lost training and racing time in Thoroughbreds. “Bucked shins” has been extensively (and variably) described in the lay and medical literature. Dorsal cortical injury in young Thoroughbreds is a result of some unknown product of the number and amplitude of loading cycles applied to their metacarpi during race horse training at high speed [8]. It is also evident from clinical experience and published data that geometric changes of the metacarpi consequent to training and maturation will lead to bones with improved mechanical properties capable of withstanding the “normal” cyclic loading of a Thoroughbred racehorse.

In horses, incomplete dorsal cortical fracture of the left third metacarpal bone occurs predominantly in flat racing Thoroughbreds. Treatment such as osteostixis alone can lead to healing, but a combination of screw placement and osteostixis is considered by some to be an additional treatment option.

2.2 Bone Handling and Preservation:

The biomechanical properties of bone vary with age, health and anatomical site. In addition, the preparation and storage of bone specimens can also affect the mechanical properties of the bone [9]. When a bone specimen is isolated from its blood supply, and no alternative sources are taken to provide for the viability its cells, the cells will die in a matter of hours, which causes change in mechanical properties. Greenberg et al. [10] non-destructively tested intact skulls and tibias within living, anesthetized dogs and again immediately after killing the animal for structural stiffness changes. It is found that the effect of death on structural stiffness was insignificant (2% maximum). Gustafson et al. [11] found that storing equine bone specimens in normal saline at room temperature for 10 days diminished their bending stiffness by 2.4% and storing in saline buffered with $CaCl_2$ prevented such changes.

There are different kinds of preservation techniques: Freezing and various Chemical Preservations using Formalin, Ethyl Alcohol and Embalming [12]. Literature review of all the above mentioned techniques are discussed in detail in this subsection.

2.2.1 Freezing of Bone:

Freezing allows the ability to store bones without any changes in mechanical properties [54]. However, there is evidence in some reports that this may not be the case. Pelker et al [13] tested rat femur specimens stored at -20, -70 and -196˚C. He found that elastic modulus and failure stress is significantly higher while freezing at -20 and -70˚C, while it is less significant in case of -196℃. In contrast to that, Frankel et al. [12] states that storing the proximal femur specimens at

-25˚C did not affect structural strength. Similarly, Goh et al. [14] states that there is no significant change in bending and torsional properties of feline humeri and femora when stored at -20˚C for 21 days. However, Linde et al. [15] states that the mechanical behavior of bone changes with time.

2.2.2 Chemical Preservation of Bone:

Chemical preservation is mostly used to prevent tissue decay, but also to preserve the cell structure for microscopic examination. The chemical solutions used for preserving the biomaterials/specimens include ethyl alcohol, glutraldehyde, formalin, phenol, glycerin and saline. Sedlin et al. [16] tested preserving the cortical bones machined from human femur in 40% ethyl alcohol, and found that the flexural modulus increases by 4%. With increase in alcohol content in the preservation solution, studies by Ashman et al. [17] and Linde et al. [15] found that there is a decrease in elastic modulus and a significant increase in hysteresis energy by 34%. Use of ethyl alcohol is suggested as better than formalin, but formalin is better in preserving the cell membranes. According to Weaver et al. [18] and Goh et al. [14], the stiffness of the bone increases by around 10% when ethyl alcohol is used. Although it is concluded that the formalin fixation produces slightly stiffer bones, the difference was not significant, especially when the formalin was buffered and made neutral.

2.2.2 Embalming of Bone:

Embalming is the technique of preserving biomaterials by treating them in chemicals to forestall decomposition. Calabrisi and Smith et al. [19] investigated the embalming effects on cortical bone of humans and found that the mean compressive strength decreased by 13%. Mcelhaney et al. [20] investigated the effect of embalming on the mechanical properties of bovine cortical bone, and found that there is a reduction of 12% in compressive strength. Porta et al. [21] studied the effect of embalming on human cadaver, and found that bone fragmentation decreased.

2.3 Bone Machining

2.3.1 Orthogonal Bone Cutting

Bone cutting is done in orthopedic surgeries for pin insertion and plate fixation when a bone is fractured. Orthogonal cutting of bone is often introduced to investigate cutting characteristics such as forces, chip formation and surface quality with respect to cutting conditions. Jacobs et al. [22] showed that the cutting forces increased linearly with feed and decreased with increased rake angle in all directions with respect to osteon orientation. In 1978, Wiggins and Malkin [23] investigated cutting forces with respect to feeds, rake angle and cutting directions at a larger range. They proposed a fracture based chip formation model and correlated specific energy with surface to volume ratio of chip linearly. In 1987, Krause [24] investigated the effect of rake angle and cutting speed on the cutting forces and concluded that the cutting forces and specific cutting energy decreased when the cutting speed increased.

In 2008, Screening Design of Experiments and ANOVA were introduced by Yeager et al. [25] to distinguish the relative importance of independent variables on the normalized cutting force. However, significance level of each variable is not analyzed in their study and the trend of cutting characteristics with respect to each variable could not be identified because they used only two levels of variables. As an alternative to these experimental methods, analytical and finite element models have been introduced to estimate forces and temperature. Equivalent heterogeneous material (EHM) was adopted by Alam et al. [26] to resemble bone material, and a continuous chip formation was supposed to study cutting forces with respect to different cutting conditions. Lee et al. [27] developed a mechanistic model for predicting thrust forces and torques during bone drilling and verified the model with experiments. Merchant's analysis of orthogonal cutting was introduced by Jacobs et al. [22] to estimate cutting forces with respect to cutting direction relative to preferred osteon direction. They concluded that Merchant's analysis had limited

application to bone material based on calculation of cutting forces with the same shear stress value for all three cutting directions.

2.3.2 Bone milling

Arbabtafti et al. [28] performed several force measurement experiments to verify the accuracy of a haptic simulation of bone machining. The effects of drill angles, feed rates and spindle speeds on forces when milling bovine femurs were examined. The results indicate the relationship between milling parameters and recorded forces suggesting a similar pattern may be identified for human temporal bone milling. However, the influence of depth of cut, which is known to affect cutting forces and accuracy in industrial milling, was not examined. Plaskso et al. [29] tested forces and specific cutting energies for orthogonal milling in bovine cortical bone for the purpose of modeling and optimizing bone cutting for orthopedic surgery. The cutting parameters similar to those used in clinical practice (very high cutting velocities and shallow depths of cut) were selected. It is demonstrated that the cutting forces and specific cutting energy are significantly different from the results at lower speeds. Denis et al. [30] examined the effects of chip load and spindle speed on forces, surface flatness and temperature rise for robotic total knee arthroplasty procedures and concluded that forces increase with feed per tooth. Bast and Englehardt [31] examined manual milling forces, temperature, time of procedure, and accuracy of neurosurgeons of different skill levels using bovine scapula specimens. They compared robotic milling forces for craniotomies with a robot to that of milling forces of neurosurgeons performing the same procedure and found that the robot was faster, more accurate, and resulted in lower forces than the surgeons.

Federspil et al. [32] tested milling forces on human temporal bones and also used a robot to perform a mastoidectomy. The milling parameters required for robotic bone milling were examined by testing milling forces on two temporal bone specimens. The effect of tool rotational

speeds, cutting velocities, various path parameters and burr types were tested. A set of parameters for calvarium bone and mastoid bone (5 mm/s at 30,000 rpm in calvarium and 1 mm/s at 30,000 rpm in the mastoid) that best fit within a criterion of 10N maximum force and 60°C maximum temperature were obtained.

2.3.3 Bone drilling

2.3.3.1 Influence of drilling speed and feed rate

There has been no consistent trend on the drilling speed on bone drilling temperature suggests in the literature. Thompson [33] found that the temperature increased at 2.5 mm and 5.0 mm from the drill site with increasing speed from 125 rpm to 2000 rpm during skeletal pin insertion in vivo of human femur bone. Vaughan and Peyton [34] studied the influence of the rotational speed on temperature rise during tooth cavity preparation and found the temperature increase with the increase in drill speed. Matthews and Hirsch [35] investigated human cadaveric femora and found that increasing the rotational speed from 345 rpm to 2900 rpm did not cause significant change in the temperature during drilling. However, increase in the thrust force results in decrease in maximum temperature and their duration. They measured the effect of applied force that varies from 19.6 N to 117.6 N along with the drill speeds varying from 345 rpm to 2900 rpm, and concluded that both the temperature and time duration above 50 °C decrease as the applied load increases. These results are also proved by Augustin et al. [36] who concluded that the peak temperature during drilling decreases as the feed rate increases. Brisman [37] reported that the drill speed of 1800 rpm and load of 1.2 kg produced the same heat as with the drill speed of 2400 rpm and the load of 2.4 kg while drilling bovine cortical bone. Increasing either the speed or the load caused an increase in temperature in bone. However, increasing both the speed and the load together allowed for more efficient cutting with no significant increase in temperature. Hillery and Shuaib [38] showed that there is a significant decrease in the temperature generated during bone drilling with increasing drill speed from 400 rpm to 2000 rpm with a drill diameter of

3.2 mm. Bachus et al. [39] examined cadaveric femur and found that the duration and magnitude of maximum temperature decreased with increasing axial thrust force at 820 rpm. Nam et al. [40] found that increasing either the speed or the force resulted in temperature rise while conducting experiments on bovine ribs by applying a load of 500 g and 1000 g with a drill speed of 600 rpm and 1200 rpm. Sharawy et al. [41] conducted experiments using 4 thermocouple technology to measure the heat generated from three drilling speeds (1225, 1667, and 2500 rpm). It was found that the mean rise in the temperature, the time of drilling and the time needed for the pig jaw bones specimen to return to the initial temperature decreases as the drilling speed increases. Apart from the studies of Matthews (1972), Hillery (1999) and Sharawy (2002) concluded that there was a general agreement in the literature that the temperature increases with drill speed approximately up to 10,000 rpm.

2.3.3.2 Predrill

Drilling can be performed either in one step or multiple steps. In one step drilling, only one drill-bit of required diameter is used to produce the desired hole. In case of multiple steps drilling, small diameter drill known as predrilling is done. Later, drill diameter gradually increased from minimum to the required diameter using a number of drills. Matthews et al. [42] conducted experiments on human-cadaveric cortical bone to examine the effect of predrilling during drilling of bone and found that predrilling is a highly effective method of minimizing temperature elevation. Branemark [43] recommended incremental drilling as it gradually removed the material from the drilling site, resulting in less friction and better heat dissipation. Itay and Tsur [44] also suggested that predrilling can effectively lessen the temperature during drilling of bone. Udiljak et al. [45] investigated with the conventional drill and step drill and showed that the maximum bone drilling temperature is much lower in case of step drill as compared to conventional drill.

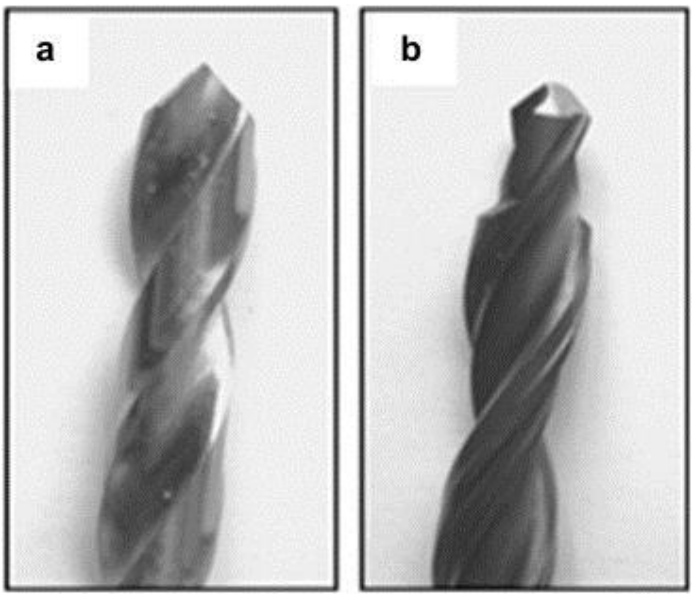

Fig. 2.2 (a) A classic surgical drill and (b) step drill (two phase drill). [45]

Kalidindi [46] also found similar results and concluded that the maximum temperature obtained using incremental drilling is significantly less as compared to single stretch drilling to produce the same hole. They suggested that it might be due to the time gap between the changes of drills during incremental drilling and hence the new drill is in cool environment as compared to the single stretch drill. They have also reported that the temperature reduction is due to the reduction in the debris buildup with step drilling. However, with predrilling, there is a disadvantage of drilling time being increased resulting in extended operation time. Recently Augustin et al. [47] examined the temperature changes in the cortical bone during drilling with a step drill. They reported no differences in the maximum bone temperature with two-step drill as compared to the standard drill bit of the same diameter.

2.3.3.3 Heat generation and temperature measurement

In orthopedics and dental practices, use of drilling process for producing holes is common. The heat is produced during bone drilling due to the plastic deformation of the bone chips, referred to as bone dust, and the friction between the bone and the drill. As bone has poor thermal

conductivity, heat is not dissipated easily, resulting in temperature rise [9]. The heat produced is a significant problem because bone is very sensitive to increase in temperature which can cause thermal necrosis. The complex relationships between the geometry of the drill bit, drilling conditions, mechanism of the chip removal and the properties of the bone presents a great challenge in developing a mathematical model for the calculation of the heat generated during bone drilling [52]. A few attempts for the development of a thermal model for bone drilling had been made. Nevertheless, mostly the theory of orthogonal cutting is applied for the calculation of the heat generated during bone drilling because the chips produced during bone drilling indicates shear failure which is similar to the chip separated from metal during machining [48] .Heat generated during drilling mainly comes from three sources (A) primary shear deformation within the shear zone, (B) friction between the rake face of the tool and the chip and (C) friction between the flank face of the tool and the newly created surface of the workpiece.

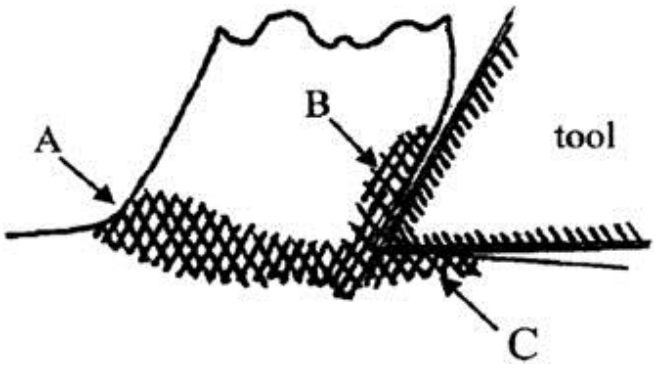

Fig. 2.3. Zones of heating in orthogonal cutting [49].

Davidson and James [49] developed an analytical model for the calculation of rate of heat entering the bone using the theory of orthogonal machining. For calculating the heat generated, they considered only the energy used for shearing of material (Zone A) by neglecting the significant effects of moving chips (Zone B), the heat produced between the tool flank and bone (Zone C) and the heat transfer between the drill bit and bone. Kalidindi [46] derived and solved the homogeneous differential equation for the heat conduction in radial direction. Tu et al.

[50] presented an elastic–plastic dynamic finite element model to simulate the temperature rise during drilling. Recently Lee et al. [51] suggested a new thermal model based on the theory of oblique cutting for applications into orthopedic surgery. All the process parameters are taken as a function of the cutting radius. They considered the cutting lips to be divided into finite number of cutting elements, each of which experiences oblique cutting mechanics. The temperature was calculated by using an explicit finite difference method.

Measurement of the temperature produced during bone drilling at the tool–bone interface is challenging. This is because of the uncertainty associated with the placement of the temperature measurement device at a certain distance from the interface. Traditional thermocouple technique has been used for the determination of the temperature elevation in both vivo and in vitro experiments (shown in figure 2.3a). Recently, use of thermographic camera has increased for the determination of the bone temperature during drilling due to ease configuration of the setup in measuring the temperature at desired location (figure 2.3b).

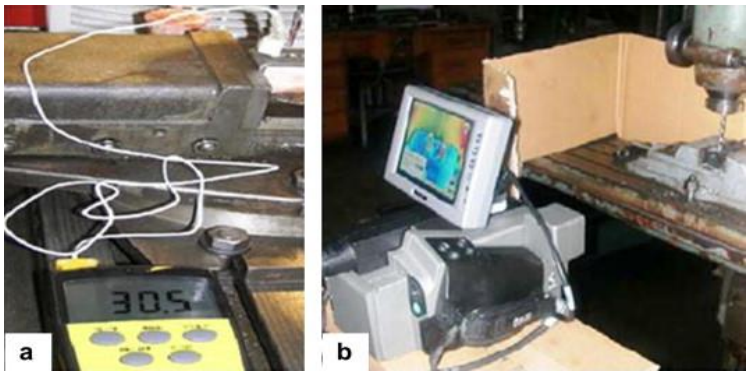

Fig. 2.4. Common methods for the estimation of temperature experimentally during bone drilling: (a) thermocouple technique[52] and (b) infrared (IR) thermography.[53]

Researchers often used two or more thermocouples for temperature measurement due to bone anisotropy. Sharawy et al. [41] used four thermocouple technique by placing thermocouples in four orientations from the hole at the same depth. Kalidindi [46] used both techniques where the

thermographic image was utilized as a template for the placement of the thermocouple. Recently Goran et al. [36] investigated the temperature distribution in drilling of the porcine femora with infrared thermographic camera. The thermographic picture shows that the temperature is the maximum along cortical bone, which is the most compact component of the bone. Both the methods are accompanied by certain disadvantages. Temperature measurement by thermocouple is not a satisfactory method because of poor thermal conductivity and inconsistent properties of bone. Also, large number of pilot holes should be prepared for thermocouple insertion during experiments. However, infrared thermographic camera only detects the surface temperature; therefore it cannot accurately predict the temperature at the actual drilling site.

2.3.4 Vibration Assisted Machining (VAM)

VAM is performed by applying high frequency and small amplitude to create a displacement between the tool and the workpiece. Due to the presence of simple cutting geometry and dynamics in turning as compared to milling, majority of the research on VAM were focused in turning. It is found that VAM has numerous advantages over conventional machining (CM), such as longer tool life [54-56], improved surface finish, burr suppression[57], and greater depth of cut for ductile regime machining of brittle materials[9] as compared to CM.

Ultrasonic elliptical vibration machining (UEVM) was first introduced in 1994 by Shamoto and Moriwaki [58]. This technique is a promising cutting method in terms of all cutting performances and has been extensively used since a decade. UEVM was used in several low machinability materials such as hardened steel [59], glass [9], and sintered WC [60]. UEVM results in smaller cutting force and longer tool life as compared to CM[59]. Numerous research works focused on the effect of cutting and vibration parameters on machining performed. The cutting force reduced in VAM due to reduced friction between the tool and the workpiece [61, 62] and the separating characteristics of the tool and workpiece [57, 63]. In previous studies, it was shown that vibration

cutting was more effective at lower cutting speed [57, 62, 63], and at higher vibration frequency and amplitude [64, 65]. It is further found that the cutting force at ultrasonic vibration cutting method is solely dependent upon the cutting speed, vibration frequency and amplitude [54, 66, 67].

In addition to turning, VAM is also used in micro-milling process to improve the cutting performance which reduced the tool wear and improved the surface quality in an aluminum alloy [68]. A two-dimensional vibration assisted micro-end milling is employed to machine the hardened steel and study the effects of vibration parameters on surface roughness and tool wear[69]. A similar work is performed on an aluminum alloy by applying an ultrasonic vibration in the micro end milling operation where vibration in feed direction resulted in reduced cutting force and uniform small chips [70]. Through the experimental results, it is predicted that the surface of the slot bottom is worse and the slot width is better when ultrasonic vibration is applied in the feed direction. The vibration assisted milling works in the past are mainly focused to investigate an effect of vibration on the cutting force [70-72], tool wear [69, 73, 74], surface roughness [69, 72, 74, 75] and tool life. However, effect of vibration assisted drilling on equine bone has not been investigated.

2.4 Investigation of Behavior of Materials and Bio-materials using Micro-CT

Micro-CT denotes Computed Tomography technique with a spatial resolution of 1 - 100μm. This is a non-destructive technique that has replaced the tedious staining techniques required by histomorphometric analysis of thin sections and other in vivo investigations on small animals. The early development of micro-CT is for the study of bone architecture and density. Recently, micro-CT has been applied in the analysis of trabecular structure, like scaffolding in fiber reinforced materials, and biomaterials.

G.Novajra et al. [76] investigated the effect of different thermal treatments and fiber diameters and length on the final scaffold structure of phosphate glass fiber. The measurement of trabecular thickness and porosity percentage for different thermal treated samples is obtained from micro-CT images. Wayne Y. Lee et al. [77] studied the effect of miR-29b-3p on mice femoral fracture healing through site-specific delivery with microbubble-ultrasound. Micro-CT is used to analyze bone volume fraction of specimen with different bone mineral densities after the injection of the compound. Balli An et al. [43] investigated the osseus integration of the titanium implants in the rabbit femur bones. X-Ray source was set to 80kV voltage and 50μA current. Pixel size resolution is 19.64μm. Figure 2.4 shows the reconstructed 3-D image of bone-implant interface from the micro-CT images.

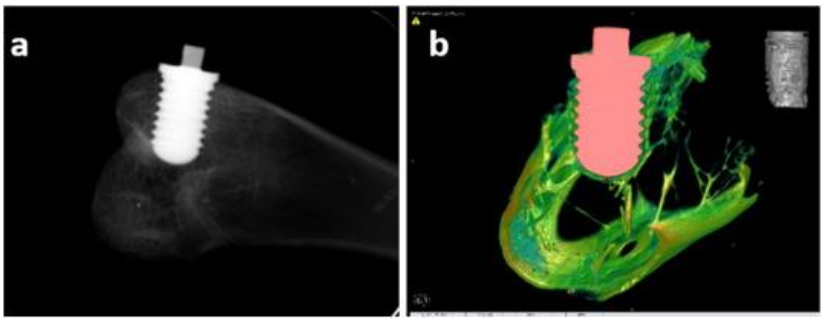

Fig 2.5. 3-D image of bone-implant interface from the micro-CT [78]

Aymeric Larrue et al. [78] analyzed the 3D morphology of micro cracks in human trabecular bone using micro-CT. Micro cracks observed in micro-CT was controlled by epifluorescence microscopy. An automatic segmentation method was used for segmenting the micro cracks in images from micro-CT, and stacks are created. These stacks were put together, known as topographic reconstruction, after which the 3D rendering of micro cracks is obtained. The automatic segmentation is again applied to the reconstructed images to observe micro crack. The process is illustrated in the figure 2.5. All these work using micro-CT suggest that the biomaterial

can be best analyzed by micro-CT and good resolution images can help identify the cracks caused by bone machining process.

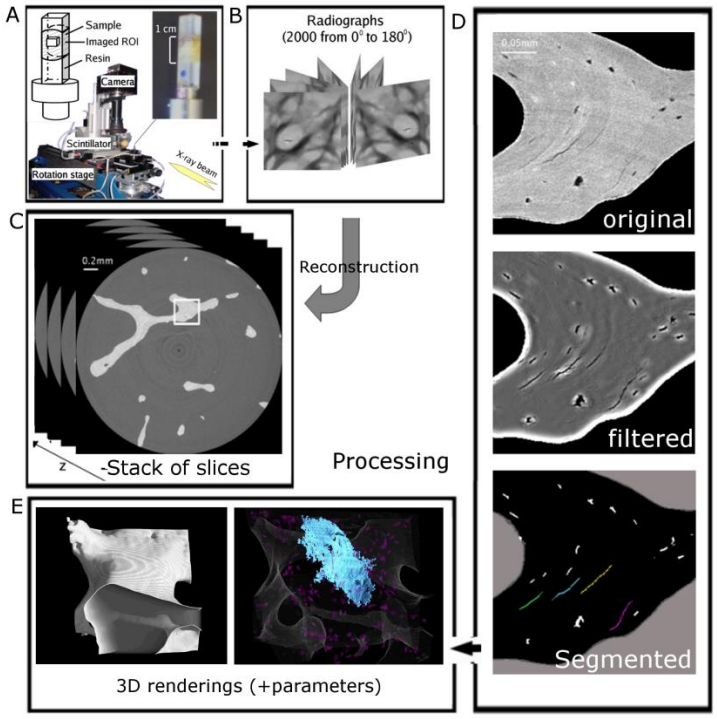

Fig. 2.6. Steps to reconstruct 2-D images from micro CT to 3-D [78]

CHAPTER 3

CONVENTIONAL AND VIBRATION ASSISTED DRILLING OF EQUINE CANNON BONE

3.1 Overview

This chapter presents the study on the effect of drilling parameters and vibration assistance on the drilling performance for equine bone. A CNC milling machine and 316L Steel Surgical drilling tool were used to conduct the experiments. A two-dimensional vibration stage with thin wall design was used to apply vibration assistance. The results of effect of the vibration on the temperature, thrust force and damages in the form of micro-cracks are discussed in detail.

3.2 Sample Preparation

Seventeen Equine cannon bones are harvested from five horses at the time of euthanasia for reasons other than for orthopedic issues. The soft tissues are removed from the bones and immediately wrapped in saline soaked towels for preventing drying and stored at -20ºC until time of use. At the time of testing, the cannon bone is thawed to room temperature and then cut into 3cm length sections using a high speed bone saw (Exact Technologies in Oklahoma City). The specimens are machined using High Speed Steel (HSS) milling tool to create 4 flat surfaces- two surfaces parallel to the long axis of the specimen and two surfaces perpendicular to the long axis of the specimen, to obtain more dimensional consistency as shown in figure 3.1.

Fig 3.1 Bone with machined surfaces

Two drilling experiments per sample are conducted. Hence, to measure the temperature during the drilling process at two different depths of 5mm and 7mm from the drill surface, two holes of 0.8mm diameter are drilled sideways on each side for depths of 5mm and 7mm, parallel to the long axis and into the cortical bone to insert thermocouples with the help of glue, as shown in figure 3.2.

a) b)

Fig 3.2 a) Two thermocouple holes, and b) Two thermocouples being stuck into the holes.

3.3 Drilling Experiments of Equine Cannon Bone

3.3.1 Experimental setup

Firstly, conventional drilling experiments are performed to investigate the effect of drilling parameters on thrust force and temperature. The equine cannon bone is machined flat on top and bottom sides. Straight holes of diameter 0.8mm are drilled, right and left, for placing thermocouple holes at distances of 5 mm and 7 mm from the top surface. A commercial MDA precision machining center is used to perform the machining experiments. Figure 3.3 shows the machining center and the experimental setup, along with the system for collecting force and temperature data. A Kistler make 9257A type sensor that is able to measure a maximum force of 5000N in all three directions is used in this project. The thermometer used for measuring temperature is an Omega HH801B, which can measure a range of -200˚C to 1372˚C. The K type 5TC-TT-K-36-36 thermocouples used (Omega) are able to sense a maximum temperature of 1200˚C and a minimum temperature of -250˚C respectively. A mist coolant setup was used to provide a continuous supply of 0.9% veterinary grade saline (NaCl) for irrigation at 60ml/min to reduce thermal necrosis in all drilling experiments.

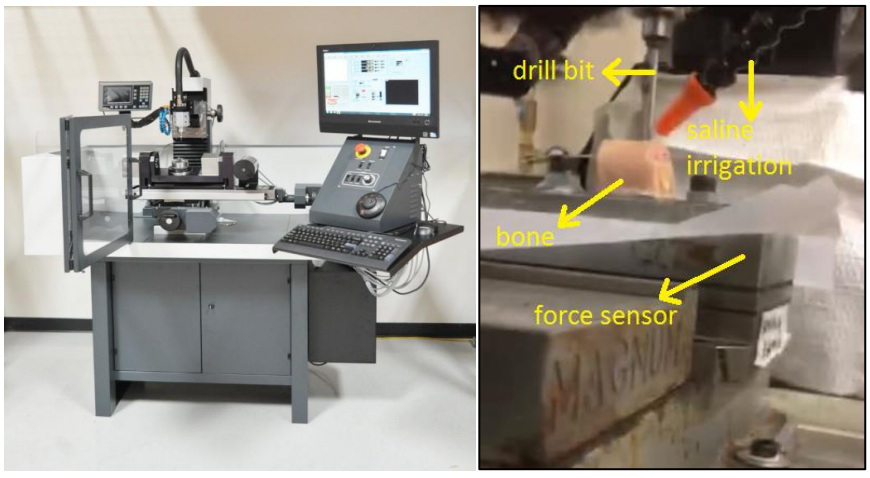

a) b)

Figure 3.3 a) MDA precision machining center and b) Experimental setup

The drill bits used for the experiment are 3.2mm diameter and 130mm long surgical drill bit manufactured by Synthes. It is made of 316L surgical steel, with a core diameter of () and the flute has helix angle of 20 degrees with the length of 38mm. The total length of the surgical drill bit was reduced from 130mm to 78mm for use in the 3 axis CNC machine. Its length is decreased to reduce the wobbling (flexing) in drilling operation (figure 3.4). Twenty drilling experiments are performed using one drill bit.

Fig 3.4 Drill bit used for bone drilling. Drill bit of reduced length is shown on the right - to minimize wobbling (flexing) during drilling.

Drilling experiments are conducted at four different spindle speeds of 5000, 7000, 40000 and 60000 rpm and four different feed speeds of 5, 10, 30 and 50mm/min. Three experiments are conducted per drilling condition for repeatability and 60ml/min flood coolant has been used to reduce the occurrence of thermal necrosis.

3.3.2 Experimental setup and Procedure for Vibration Assisted Drilling

A two dimensional vibration stage with thin wall design, attached with two piezo actuators is used for providing vibration during drilling. The trunnion system of the MDA CNC machine is used to hold the vibration stage at 90 degrees, so that one piezo acts as z-axis vibration source. An L-clamp is fastened on to the vibration stage, upon which bone is clamped as shown in figure 3.5. Drill bit, force sensor, thermometer and thermocouple used in this setup are of the same specifications as in conventional drilling.

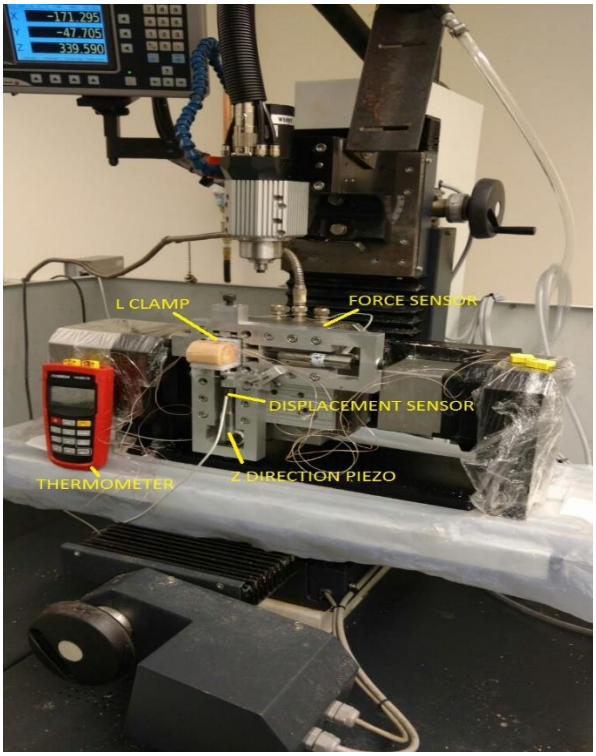

Fig. 3.5 The vibration assisted drilling experimental setup

The experiments are conducted on the bones for 5 different spindle speeds of 5000, 7000, 10000, 40000 and 60000 rpm and four different feed speeds of 5, 10, 30 and 50mm/min to characterize the behavior of temperature and thrust force in low and high spindle speed and feed speed. Similar to the conventional drilling, 60ml/min flood coolant of 0.9% veterinary grade NaCl

Saline is used during the experiments to reduce the thermal necrosis and each experiment is repeated three times for repeatability. The vibration frequency is kept constant at 8160Hz and the corresponding amplitude is 40microns. Some experiments are conducted for 20mm/min feed speed as well for better understanding of behavior of temperature and force. The depth of drilling is kept constant at 20mm from top surface of the specimen.

3.4 Results and Analysis

3.4.1 Dimensional consistency of hole:

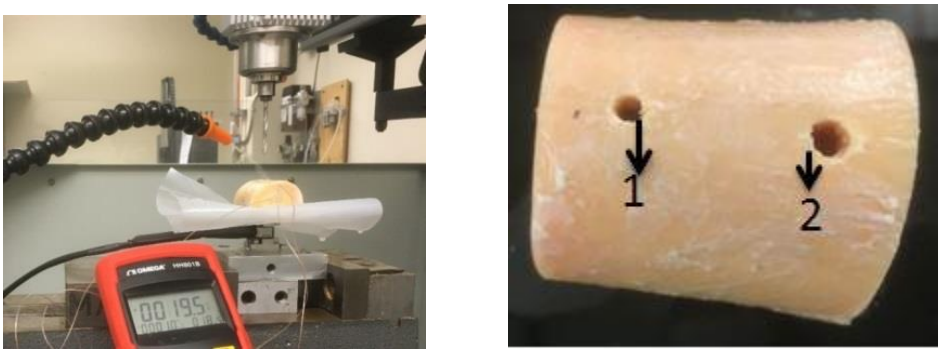

(a) (b)

Figure 3.6 (a) Setup of Bone Drilling Experiments (b) Geometry of Drilled Holes.

From the three experiments performed for each drilling condition, it is found that the diameter of the hole is enlarged at the bone surface as a result of the drilling process. The measurement of the hole diameter was performed at the surface of the hole using a Mitutoyo Vernier Caliper with a least count of 0.001mm. The diameter is measured at three different places along the circumference of the hole, and the average is documented.

The figure 3.6b shows two enlarged holes. The hole marked 1is caused by 40000 rpm and the hole marked 2 is caused by 60000 rpm. For spindle speeds of 40000 and 60000 rpm, at feed speed of 30mm/min, the maximum surface diameter of drilled holes measured 3.85mm and 4.85mm respectively. For feed speed of 5mm/min, it measured 3.45mm and 4.5mm respect4ely. The vibration assisted machining for same drilling conditions does not improve the geometry of the hole, as the maximum surface diameter at feed speed of 30mm/min measured 4.05mm and 4.93mm for 40,000 and 60,000 rpm respectively. It is because of the increased wallowing of the drill bit due to the applied external vibration. Variation in drill hole diameter is shown in the Figure 3.6. The enlarged surface diameter of the hole observed in the figure above might be because of the high vibration of drilling tool at higher spindle speeds due to the large overhanging length. This also implies that the overhanging drill length has a significant effect on the drilled hole diameter at higher spindle speeds.

3.4.2 Temperature:

Figure 3.7 shows variation in temperatures for constant spindle speed and different feed speeds:

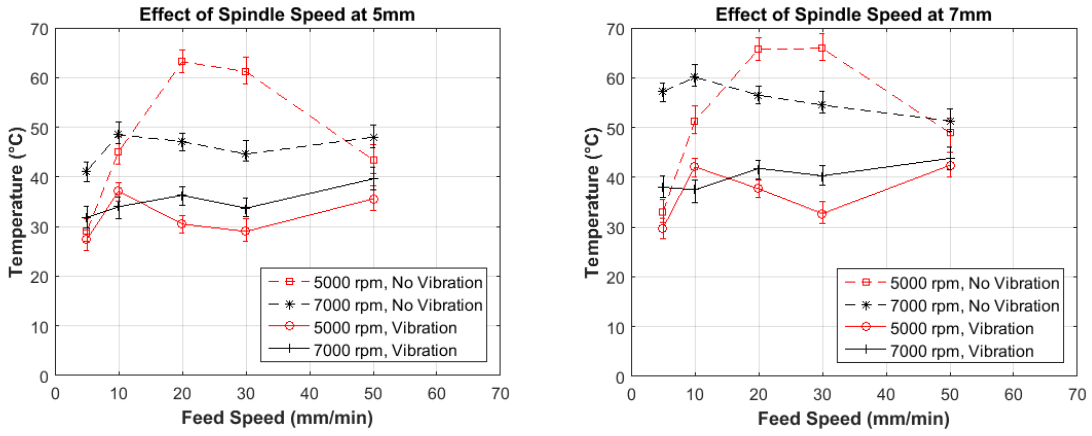

a) b)

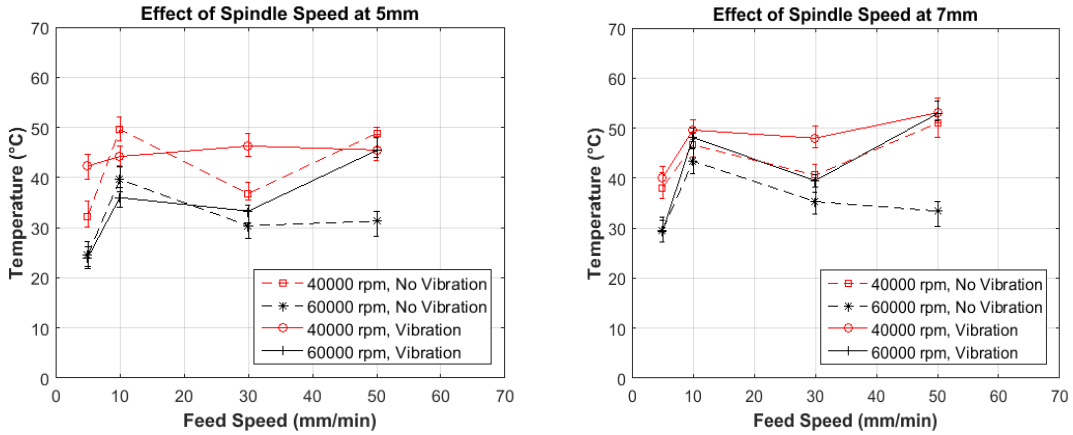

c) d)

Fig 3.7. Graphs showing variation of Temperature at different feed speeds and constant spindle speed

In all the graphs above, it can be observed that, for constant spindle speed and increase in feed, there is increase in temperature from 5mm/min to 10mm/min because of increasing friction due to sliding contact (rubbing) because of low speed machining. It is also evident that there is decrease in temperature from 10mm/min to 30mm/min, as there is more cutting mechanism taking place than rubbing, which reduces the friction. The increase in temperature form 30mm/min to 50mm/min is because of the high deformation happening due to larger chip load. Also, another fact that can be observed is that, temperature at 7mm depth is higher than temperature at 5mm due to heat accumulation. The temperature for vibration assisted drilling is found to be less than the conventional drilling because of the intermittent cutting process happening instead of the continuous cutting process.

Figure 3.8 shows variation in temperature for same feed speed and different spindle speed. When the feed rate was kept constant, an increase of tool rotation speed led to an increase in sliding distance between tool and the workpiece within a fixed period of time. This is the reason why the cutting temperature increases as spindle speed increased from 5000 to 40000rpm. Decrease in

temperature from 40000 rpm to 60000 rpm is because of hole enlargement leading to saline irrigation reaching the depths of hole, which resulted in temperature decrease.

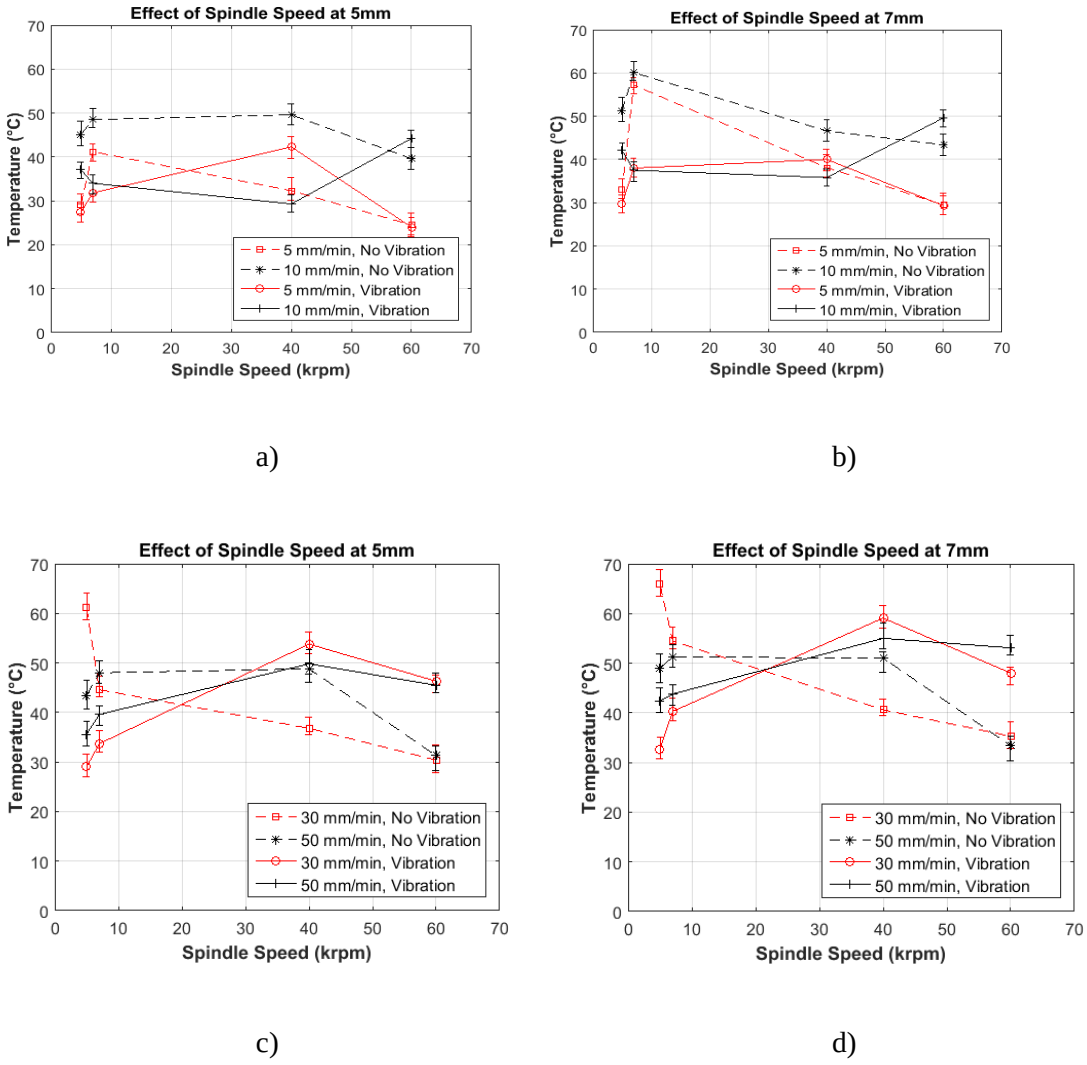

Fig. 3.8. Graphs showing variation of Temperature at different spindle speeds and constant feed speed

For the vibration assisted drilling at 10mm/min, temperature at 60000 rpm is higher than 40000 rpm, defying the overall trend. It is because, the wobbling tool at high spindle speed makes contact with the thermocouple directly, that causes hike in temperature. It can also be observed that the temperature of the vibration assisted drilling is less than that of the conventional drilling.

It is because of the fact that the vibration assistance makes the drilling process intermittent instead of continuous, which reduces the friction.

3.4.2.1 Variation of Temperature with time during thermocouple measurements:

In this section, variation of temperature during the measurement using thermocouple is discussed. Thermocouples are placed at 0.5mm from the drilling tract by inserting them at 5mm and 7mm in the sites. Figure 3.9 shows the variation of temperature at 50mm/min for different spindle speeds with and without vibration assistance at 5mm depth.

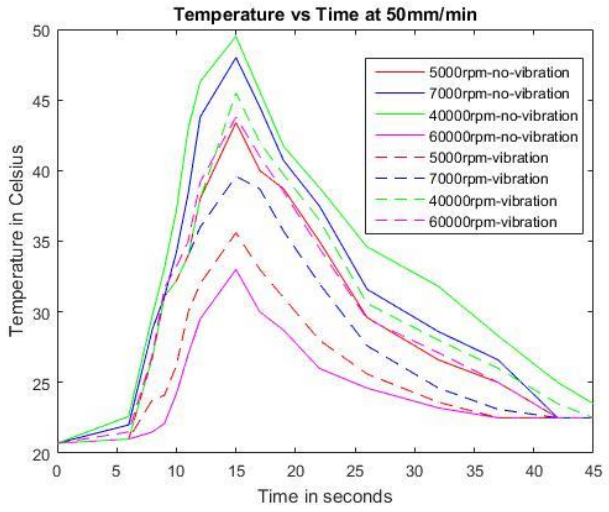

Fig 3.9. Temperature vs Time at 50mm/min and different spindle speeds with and without vibration assistance

No significant temperature rise is recorded until the cutting edge approached the location where the thermocouples are placed. It may be due to the low thermal conductivity of the bone. This is the reason behind the quick rise and fall of temperature seen in the figure. The same trend is followed at 7mm depth as well, while the magnitude is different because of heat accumulation.

The figure 3.10 shows the variation of temperature at 7000rpm for different feed speeds. The time taken by the drilling process at different feed speeds is evident from the graph. Also, the peak temperature is achieved more quickly at higher feed speed due to higher process speed.

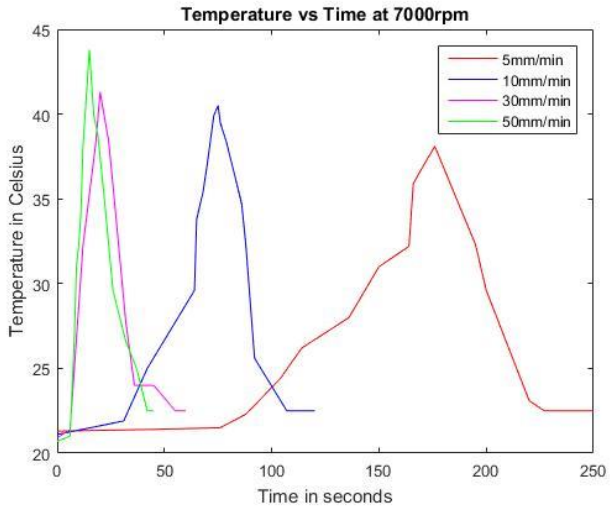

Fig 3.10 Temperature vs Time at 7000rpm and different feed speed

3.4.3 Thrust Force

Thrust force graphs with constant spindle speed are shown in figure 3.11.

The x axis is feed speed in mm/min and y axis is thrust force in N. The graphs below show that the thrust force increasing with increase in feed speed at all spindle speeds except for 40000 and 60000 rpm at 50mm/min in conventional drilling. At these particular drilling conditions, rupture caused in bone initially makes the tool-workpiece contact irregular, resulting in less force. In case of vibration assisted drilling, the thrust force is less in case of higher feed rate, because the external vibration results in a lower depth of cut for each tooth on the tool due to the intermittent contact.

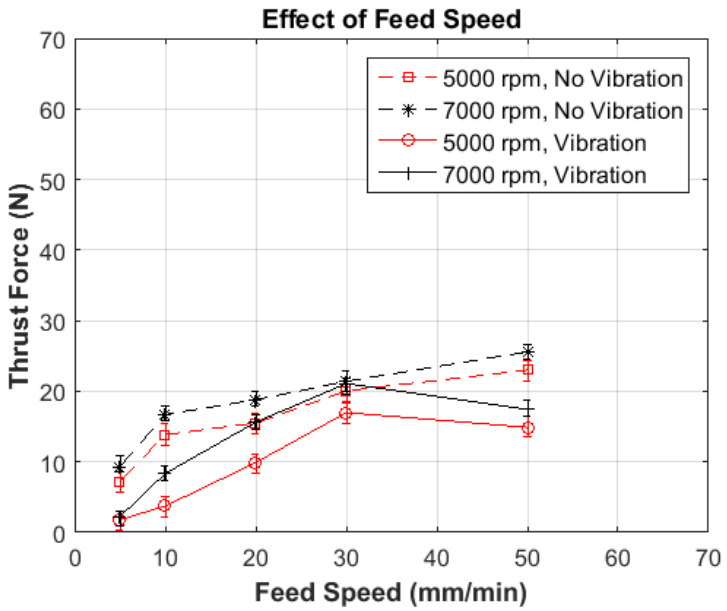

a)

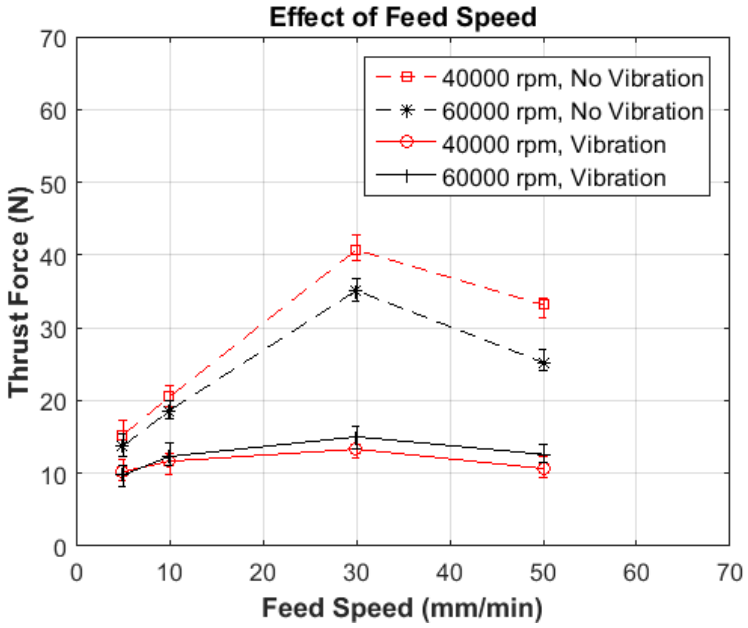

b)

Fig. 3.11. Graphs showing variation of Thrust force at different feed speeds and constant spindle speed

Figure 3.12 shows thrust force versus spindle speed with feed speed as constant. From the graphs, it can be conceived that the thrust force increases with the increase in spindle speed because of more sliding contact with increased tool rotation. However, the thrust force decreases from 40000 to 60000 rpm in case of cannon bone because of the wobbling of drill bit, and the damage caused because of that. This rupture results in enlarged holes, which reduces the tool- workpiece contact. It is also evident that the vibration assisted drilling has less thrust force when compared to the conventional counterpart because of the drill bone contact becomes being intermittent instead of continuous.

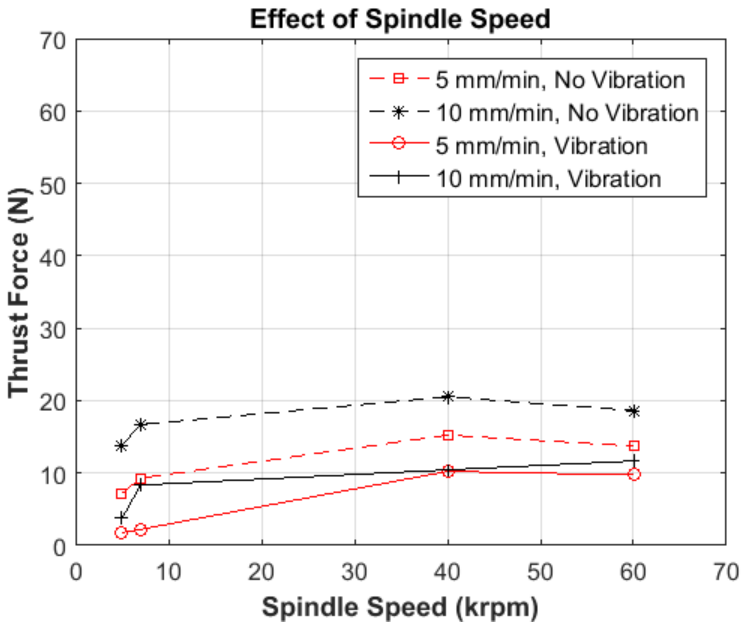

a)

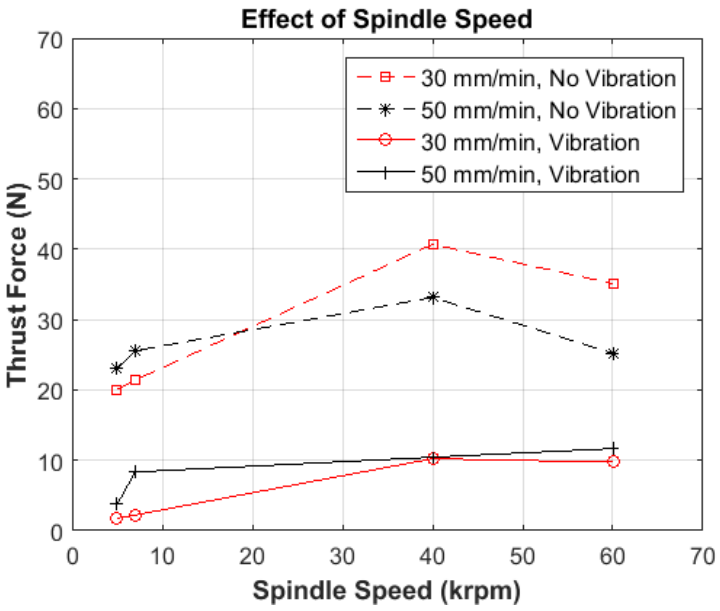

b)

Fig.3.12 Graphs showing variation of Thrust force at different spindle speeds and constant feed speed

3.4.4 Comparison of drill wall images from Micro-CT

The regions of the drilled hole in the samples are scanned in micro-computed tomography (micro-CT) in Skyscan 1172 model at 11.76µm resolution, 87kV voltage and 120µA current. The samples are cut into small pieces of approximately 24mm in height and width, as shown in figure 3.13a, in order to increase the resolution of the images. The Skyscan 1172 system as shown in figure 3.13b, has x-ray source on right side and the detector is on left side of the machine. Medium camera of 2000*1048 pixels is chosen to scan the whole specimen. The specimen is mounted on micro-CT stage for scanning as shown in figure 3.13c.

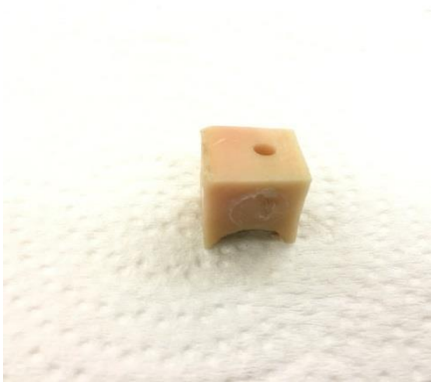

a)

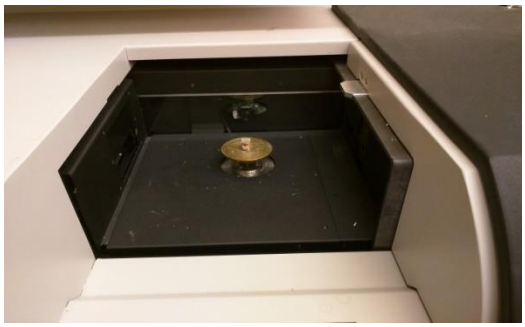

b) c)

Fig.3.13 a) Downsized sample for scanning b) Skyscan 1172 microCT equipment

c) Sample mounting stage

900 images are obtained for each sample. One image is generated for every 0.4 degree rotation of the sample. Images are saved in the 16 byte TIFF format to retain overall detail. These images are reconstructed using software called NRecon. Misalignment, ring reduction and beam hardening are the parameters employed to enhance the images to retain the details. The reconstructed images provide cross-section images of the specimen, where the wall of the drilled hole can be seen as shown in figure 3.14.

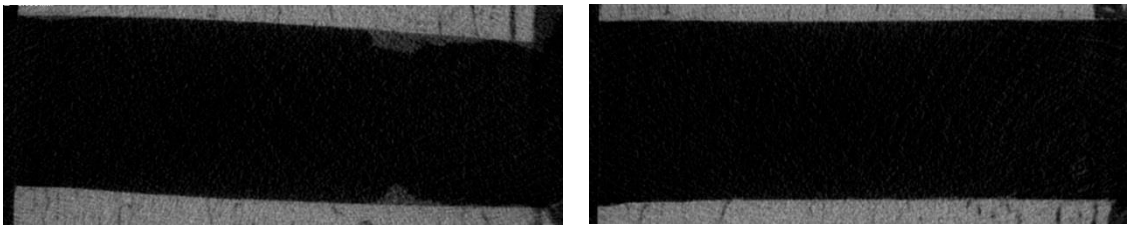

a) 5000 rpm and 10 mm/min no vibration and with vibration

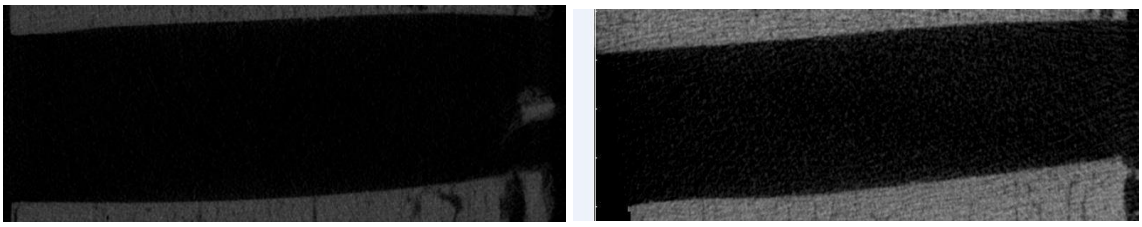

b) 5000 rpm and 30 mm/min no vibration and with vibration

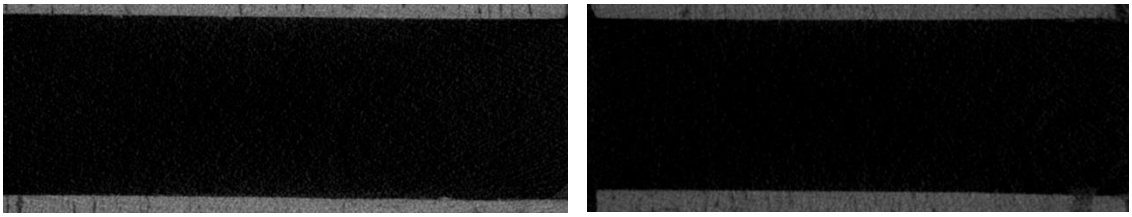

c) 7000 rpm and 10mm/min no vibration and with vibration

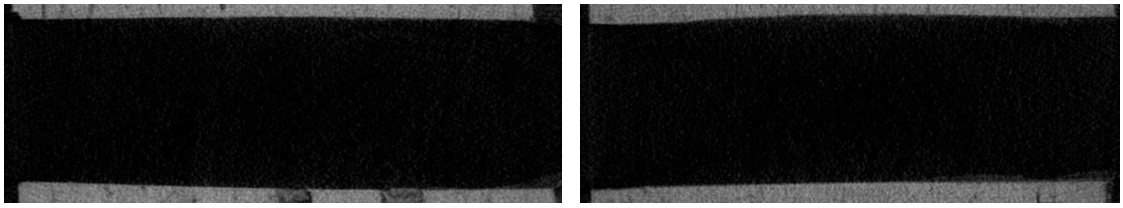

d) 7000 rpm and 30 mm/min no vibration and with vibration

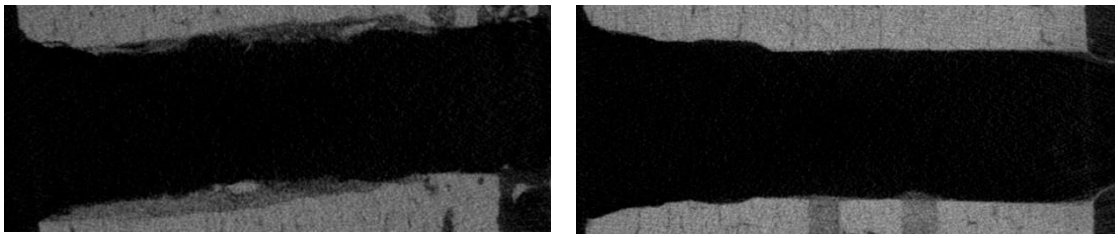

e) 60000 rpm and 10 mm/min no vibration and with vibration

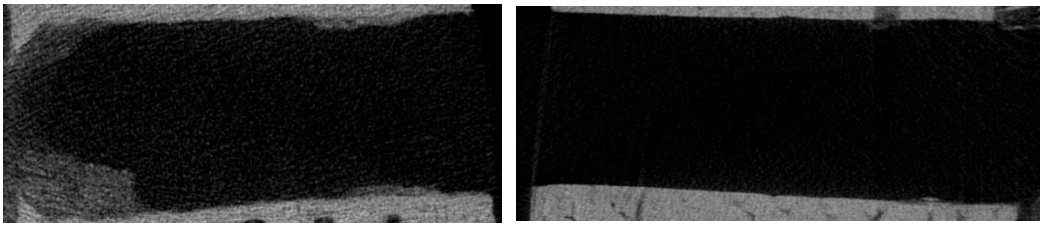

f) 60000 rpm and 30 mm/min no vibration and with vibration

Fig.3.14 Drill hole quality observation form reconstructed micro-CT images.

From the figure 3.14 e and 3.14 f, it is evident that the drill wall is not straight and the diameter is not maintained throughout. This is because of wobbling of the drill bit occurs at higher spindle speed such as with 60000 rpm. Moreover, it can be observed that chunks of materials are attached to the wall of 60000 rpm at 10mm/min and 60000 rpm at 30 mm/min with no vibration because of wobbling drill bit, as there is most likely no frequent tool contact with the wall. Although the hole diameter is not consistent throughout with the vibration assisted drilling; however, there is no material attached to the wall. This may be due to vibration in z axis direction along with the wobbling of tool creating a larger diameter (elliptical path). In addition, walls appear cleaner due to its frequent contact with the tool. It is noticeable in figures 3.14a to 3.14c that the walls are clean and straight at lower spindle speeds, except for debris remaining in the no vibration specimens. It can also be observed that at 60000 rpm and 10mm/min, more uncut material is adhering to wall compared to 60000 rpm and 30mm/min. It is caused by extensive micro-fracture occurring with lower drilling speed. Therefore, it can be concluded that the vibration assisted drilling provides improved results compared to conventional drilling at higher spindle speeds.

CHAPTER 4

MILLING OF BOVINE CANNON BONE

4.1 Overview

In this chapter, the investigation on effect of slot milling parameters including spindle speed, feed per tooth and depth of cut on cannon bone's surface roughness, milling forces on both x and y directions and temperature is discussed. Taguchi method is used to find the most deterministic parameter on surface roughness, force and temperature.

4.2 Sample Preparation

Bovine cannon bones are prepared the same as described for the equine canon bones and stored at -20ºC. The cannon bones are cut into 3cm sections for testing using a precision bone saw as shown in figure 4.1a. The bone sections are machined flat on top and bottom of the cortical bone (hard part) as shown in figure 4.1b. These machined pieces are taken to Exact Technologies for sectioning the specimens into two halves (cross-sectionally) and creating grooves in one of the half sections to accommodate thermocouples in them (figure 4.1b). Marrow is removed from the cut sections and thermocouples are implanted at a calculated distance from the surface, so that the tool's tip comes within 0.5mm from the thermocouple. Epoxy is then prepared and poured into the marrow cavity. The specimens are left to cure for 8 hours wrapped in saline soaked towel at room temperature.

a) b)

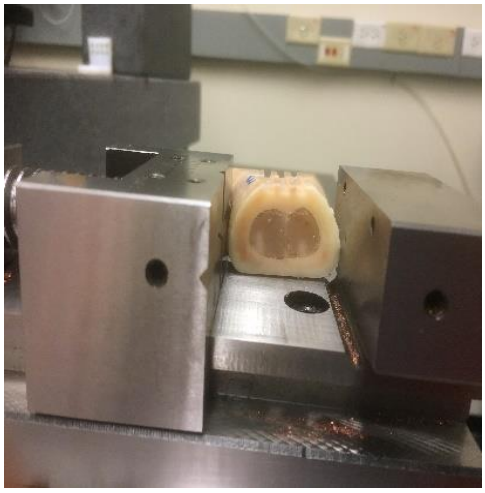

c)

Fig.4.1. a) The pathological saw, b) The grooved half of bovine cannon bone and c) The epoxy filled bone.

4.3 Experimental Setup

A commercial MDA precision micro milling machine was used for the experiment. Its maximum spindle speed is less than 60,000 rpm. A four-flute High Speed Steel (HSS) end mill (MICROCUT) with 1/8 in (3.175 mm) diameter and 30º helix angle was used. Kistler 9317c

dynamometer was used to measure force. It can measure a maximum force of 500N in all three directions. The bone is directly clamped to the Kistler 9317c force sensor, by drilling a 2.6mm hole and tapping a 3mm bolt to it. Both x and y direction force due to milling operation is measured. The temperature is measured using Omega HH801B thermometer, and a K type 5TC-TT-K-36-36 omega thermocouple. This temperature measuring setup can measure any temperature between -200 ˚C to 1372 ˚C. After the experiments, surface roughness is measured using Mitutoyo SJ 210.The experimental setup and the surface roughness tester is shown in the figure 4.2b.

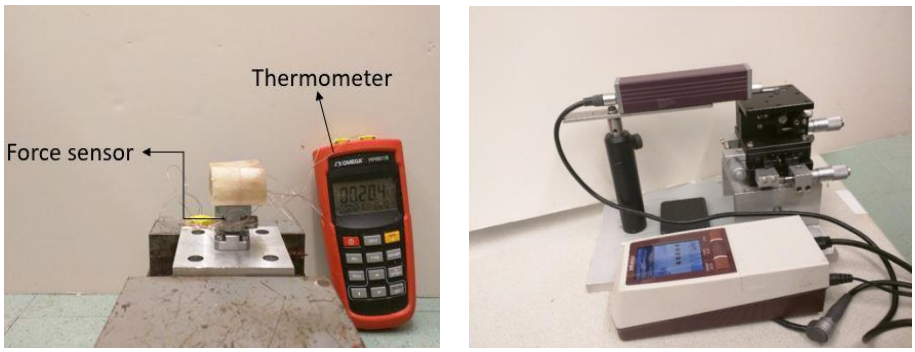

a) b)

Fig.4.2. a) Experimental setup b) Surface Roughness Tester SJ 210

4.4 Experimental Procedure

Design of Experiments is used to design a 3 factor 4 level orthogonal matrix list to reduce the number of experiments from 64 to 16 as shown in table 4.1. The 3 factors are spindle speed, feed per tooth and depth of cut.

Speed (RPM)	Feed per tooth (mm/min)	Depth of cut (mm)	Fx (N)	Fy (N)	Temp (celsius)	Roughness (microns)
6000	0.1	0.5	4.63	5.1	23.2	1.41
6000	0.2	0.75	27.9	19.1	23.5	0.38
6000	0.3	1	24.52	25.32	25.5	0.83
6000	0.35	1.5	10.33	12.61	34.0	0.82
8000	0.1	0.75	10.25	12.91	28.6	0.23
8000	0.2	0.5	14.79	18.72	24.6	0.77
8000	0.3	1.5	20.72	27.28	27.7	1.13
8000	0.35	1	18.28	17.87	26.1	1.05
10000	0.1	1	10.46	17.32	29.8	1.81
10000	0.2	1.5	14.18	16.70	25.7	0.47
10000	0.3	0.5	23.19	29.54	24.5	0.61
10000	0.35	0.75	22.79	35.99	23.4	0.53
15000	0.1	1.5	21.51	19.38	30.9	0.55
15000	0.2	1	20.51	25.83	25.4	0.81
15000	0.3	0.75	21.28	18.36	24.3	0.94
15000	0.35	0.5	19.31	25.51	23.6	0.66

Table 4.1 Results of Temperature, Cutting forces and Surface roughness obtained from the 16 milling experiments

4.4.1 Analysis of the results using Taguchi Method

Once the results were obtained, Taguchi method was used to analyze the degree of influence of each factor for each of the responses including force in x and y direction, temperature and Surface roughness. Taguchi method has two types of problems: Static and Dynamic. The problem in this study is static in nature.

4.4.1.1 Static Problem

Generally, a process to be optimized has several control factors which directly decide the target or desired value of the output. The optimization then involves determination of the best control factor levels so that the output is at the target value. Such a problem is called "Static Problem".

This is best explained using a P-Diagram which is shown in figure 4.3. ("P" stands for Process or Product). Noise is shown to be present in the process but should have no effect on the output. This is the primary aim of the Taguchi experiments - to minimize variations in output even though noise is present in the process. The process is then said to have become ROBUST.

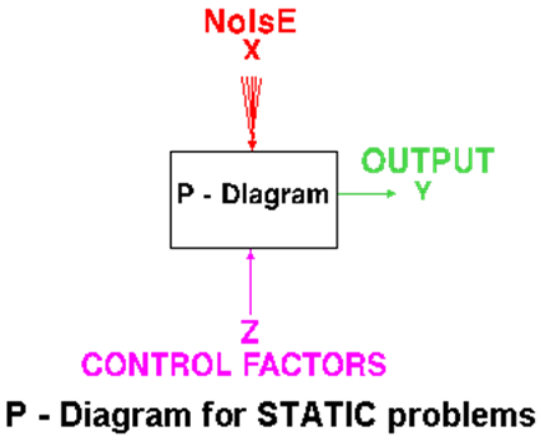

Fig.4.3 Schematic diagram for static problem

There are 3 Signal-to-Noise ratios of common interest for optimization of Static Problems;

1) Smaller the better:

$$n = -10\log_{10}[\text{mean of sum of squares of measured data }]$$

2) Nominal the best,

$$n = -10\log_{10}[\text{mean of sum of squares of reciprocal of measured data }]$$

3) Larger the better

$$n = 10\ \log_{10}\frac{square\ of\ mean}{variance}$$

Taguchi method is accomplished using Minitab 15. The following are the results from Minitab 15.

4.4.1.2 Signal to Noise ratio graphs for each response:

SURFACE ROUGHNESS

Smaller is better – As smoother surface ensures precise attachment of artificial implants.

Level	Spindle Speed (rpm)	Feed per tooth(mm/tooth)	Depth of cut (mm)
1	2.1464	2.3383	1.766
2	3.3207	4.6877	6.6625
3	2.7477	1.3307	-0.5727
4	2.7083	2.5665	3.0673
Delta	1.1743	3.357	7.2353
Rank	3	2	1

Table 4.2 Response Table for Signal to Noise Ratios for surface roughness

Depth of cut is the most influencing parameter for surface roughness output. The reason may be, as the depth of cut increases the contact of flank face of the tool increases. The deformation is

high due to more shear. This leads to increase in friction and heat production in the process [79]. This results in more damage to the surface because of more sticking contact than sliding in the flank face. Feed rate and spindle speed are not as dominant as depth of cut because the analytical evaluation by Yeager et al proves that and, the larger depth of cut also produces larger debris which results in re-deposition on bone matrix causing irregularity in surface, which does not depend on feed rate or spindle speed . [25].

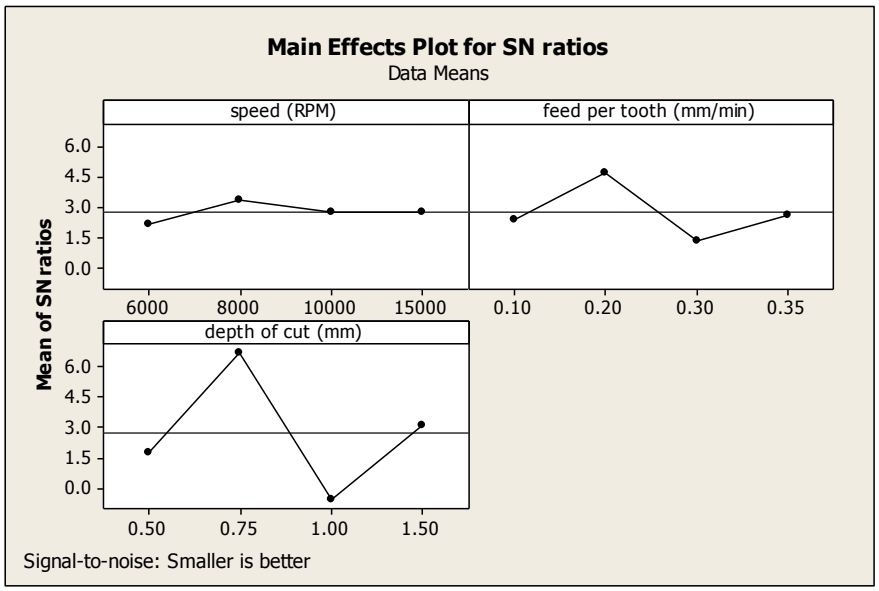

Fig 4.4 Main Effects plot for SN ratios- roughness

TEMPERATURE

Smaller is better – Lower operating temperature is preferred to prevent thermal necrosis.

Level	Spindle Speed (rpm)	Feed per tooth (mm/tooth)	Depth of cut (mm)
1	-28.38	-28.94	-27.6
2	-28.54	-27.9	-27.92
3	-28.23	-28.13	-28.52
4	-28.28	-28.46	-29.38
Delta	0.32	1.04	1.77
Rank	3	2	1

Table 4.3 Response Table for Signal to Noise Ratios for temperature

The most deterministic parameter for temperature response is depth of cut. The physical reason for this result is, as the area of contact of the tool increases with the bone, so does the increase in friction, producing more heat. The feed speed and spindle speed also influences the temperature, but not as much as depth of cut, because a big scale brittle fracture can occur in front of the cutting edge parallel to the cutting direction, when the cutting edge collides mechanically to the workpiece in the tool feed per tooth. So, temperature does not rise because of brittle fracture[80].

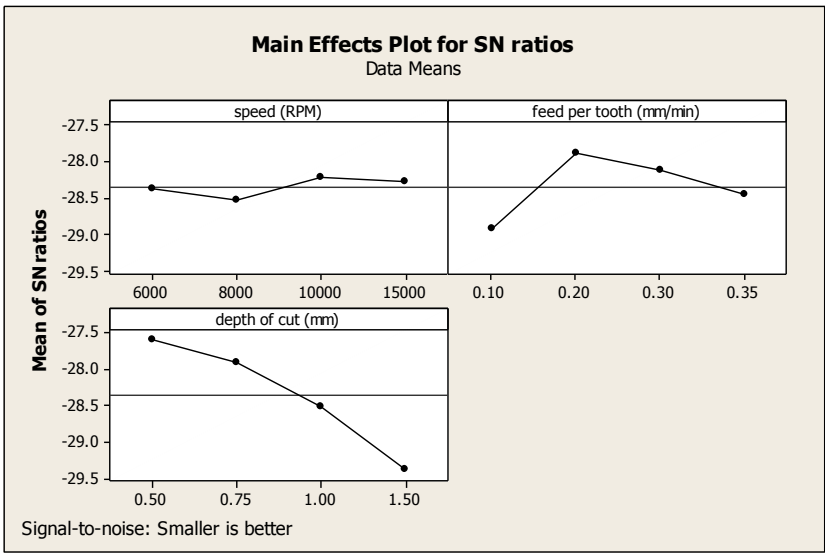

Fig. 4.5 Main Effects Plot for SN ratios- Temperature

FORCE IN X DIRECTION

Smaller is better – Lower cutting forces are preferred for longer tool life and smoother surgery (less damages during surgery).

Level	Spindle Speed (rpm)	Feed per tooth (mm/tooth)	Depth of cut (mm)
1	-22.57	-20.14	-22.43
2	-23.8	-25.4	-25.71
3	-24.47	-27	-24.92
4	-26.29	-24.6	-24.08
Delta	3.72	6.85	3.28
Rank	2	1	3

Table 4.4 Response Table for Signal to Noise Ratios for force in X direction

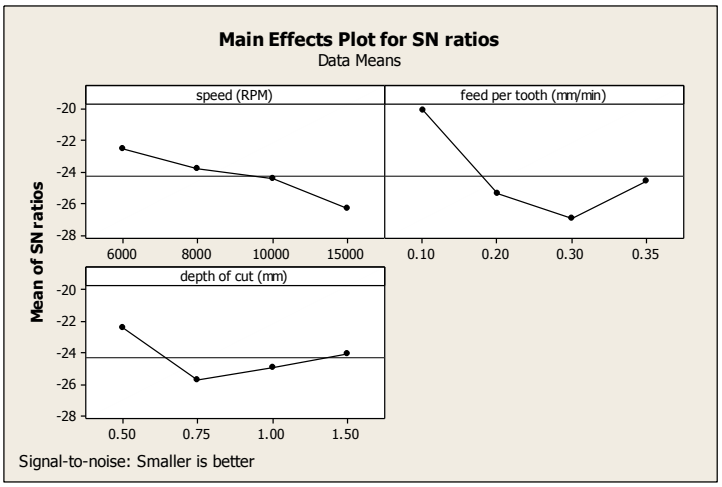

Fig. 4.6 Main Effects Plot for SN ratios- Force X direction

FORCE IN Y DIRECTION

Smaller is better

Level	Spindle Speed (rpm)	Feed per tooth (mm/tooth)	Depth of cut (mm)
1	-22.47	-21.73	-24.29
2	-25.36	-25.94	-26.06
3	-27.44	-27.87	-26.53
4	-26.85	-26.58	-25.23
Delta	4.97	6.14	2.24
Rank	2	1	3

Table 4.5 Response Table for Signal to Noise Ratios for force in Y direction

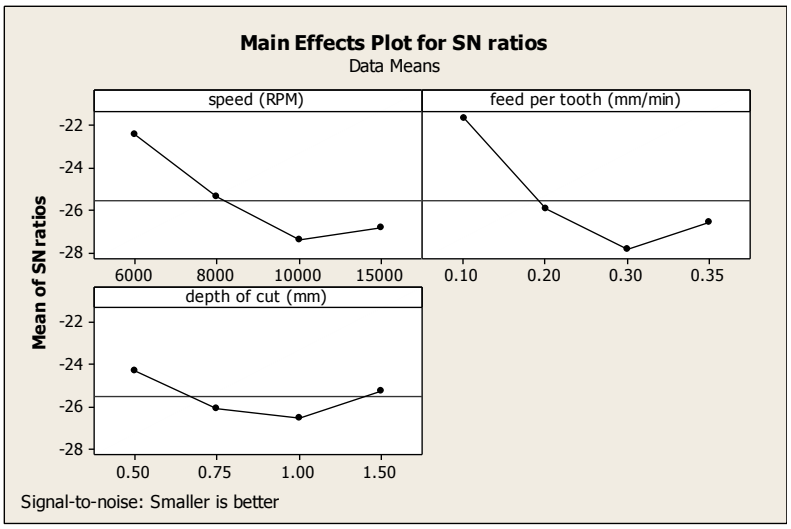

Fig. 4.7 Main Effects Plot for SN ratios – Force in Y direction

Feed rate is the most influencing factor for force output. The reason is because, the cutting force increases with increase in material removal rate. As the feed rate increases, material removal rate increases, resulting in high cutting force. Depth of cut and spindle speed are not as dominant as feed rate because, the feed rate determines the amount of material removed that directly affects the force.

Summary from Taguchi analysis:

These results convey that the most influencing parameter for Forces in x and y direction is '***Feed rate***'. Similarly, for Surface roughness and Temperature, the most influencing parameter was '***Depth of cut***'.

4.4.2 ANOVA- General Linear Model for optimum milling parameters

4.4.2.1 Response Optimizer:

Response Optimizer is a tool the software Minitab that helps in identifying the combination of input variable settings that jointly optimize a single response or a set of responses. Joint optimization must satisfy the requirements for all the responses in the set, which is measured by

the parameter called composite desirability. Composite desirability evaluates the extent to which a particular condition or setting optimizes a set of responses overall. Desirability has a range from 0 to 1, where 1 represents the ideal condition and vice versa. Mathematically, it is the weighted geometric mean of the ind4idual desirability for the responses. Minitab determines optimal settings for input variables by maximizing the composite desirability.

TEMPERATURE:

Temperature is considered the most important response. First step is to setup the response optimizer by choosing which responses must be maximized or minimized as shown in figure 4.8. Then, weight and importance is input according to the need of the scenario. Weight and Importance can be rated from a range of 0.1 to 10. For the purpose of this study, the input was given as shown in the figure, where the highest weight and importance is selected as 1, with percentage in mind.

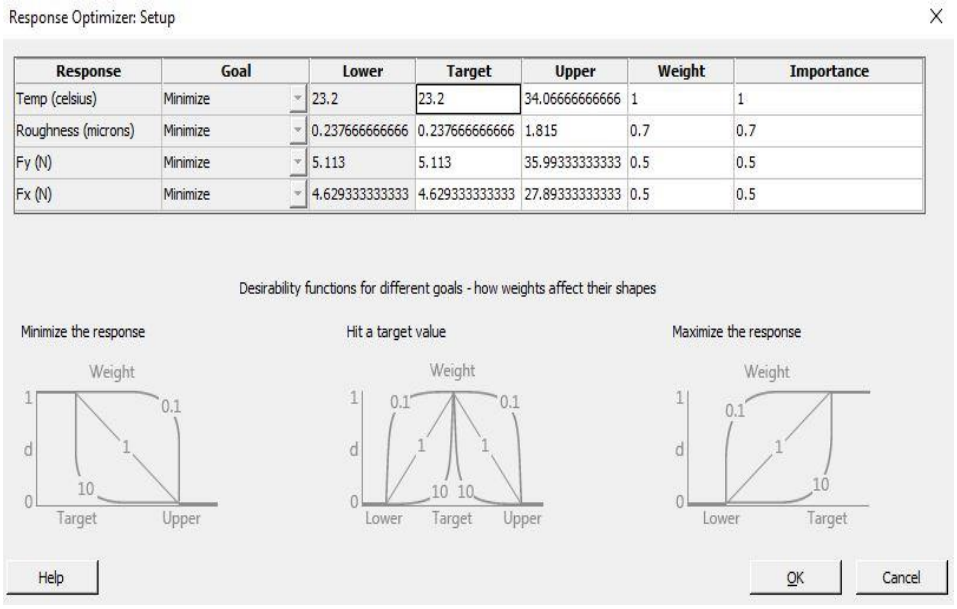

Fig. 4.8 Setup window from Response Optimizer

The next step is to select the constraints in the option, which is to mention the region of values for the variable, like holding a particular value, or constraining to a particular region. This makes the prediction of most composite desirable condition to fall in the region of interest. In this study, the options are chosen as shown in figure 4.9.

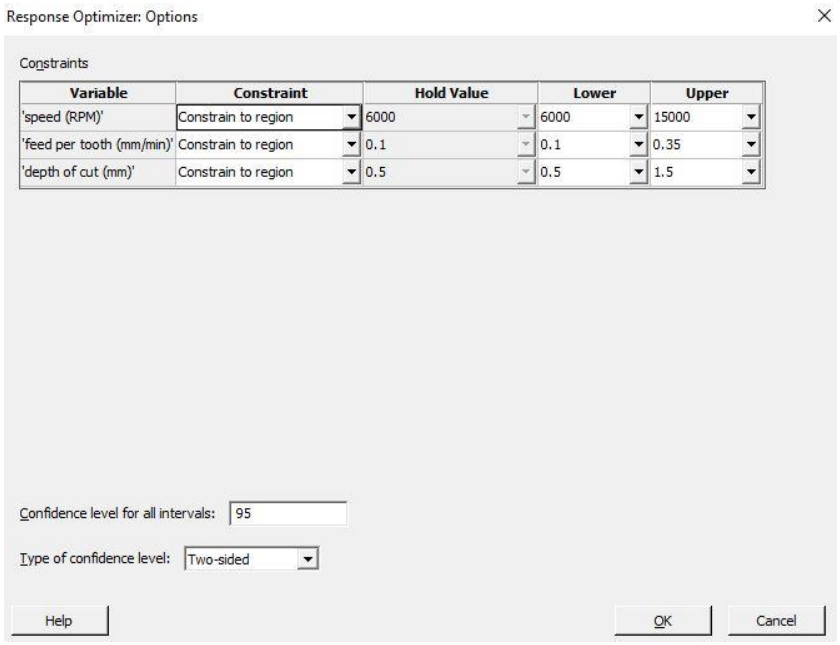

Fig.4.9 Options window from Response Optimizer.

The final step is to select the number of solutions to be displayed that has top desirability values, and perform the analysis with the given inputs. The tool provides several tables along with the plot as shown below.

Multiple Response Conditions

Solution	Spindle Speed (rpm)	Feed per tooth (mm/ min)	Depth of cut (mm)	Temp (°C)	Roughness (microns)	Fy (N)	Fx (N)	Composite Desirability
1	6000	0.2	0.5	22.77	0.70	14.40	16.08	0.852
2	8000	0.2	0.5	22.97	0.64	18.06	15.25	0.851
3	6000	0.2	0.75	22.74	0.36	16.27	21.15	0.826

a) Multiple solutions

Variable	Setting
Speed (rpm)	6000
Feed per tooth (mm/min)	0.2
Depth of cut (mm)	0.5

b) Most desirable solution

Response	Fit	SE Fit	95% CI	95%PI
Temp (Celsius)	22.78	2.18	(17.43, 28.12)	(14.16, 31.39)
Roughness (microns)	0.708	0.359	(-0.171, 1.587)	(-0.709, 2.215)
Fy (N)	14.4	5.87	(0.05, 28.76)	(-8.74, 37.55)
Fx (N)	16.08	5.17	(3.43, 28.73)	(-4.31, 36.48)

c) Table showing Confidence Interval values

Table 4.6. Output tables from Response Optimizer from Minitab.

Table 4.6 (a) shows 3 conditions that are possible overall desirable outcome, which gives minimum responses as suggested. Then, the most desirable setting is put forth by the software, which is 6000 rpm, 0.2mm/min and 0.5 mm for the temperature as priority. Figure 4.10 shows individual desirables that led to the collective/composite desirability.

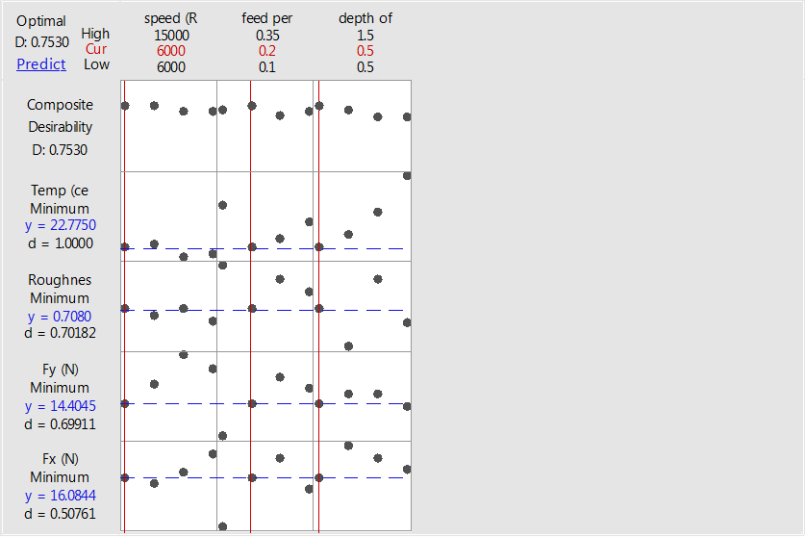

Fig. 4.10. Response Optimizer plot from Minitab

ROUGHNESS AND FORCE:

The Response Optimizer was used for both roughness and Fx, Fy individually, with importance and weight as 1 as shown in figure 4.11

Parameters

Response	Goal	Lower	Target	Upper	Weight	Importance
Temp (celsius)	Minimum		23.2000	34.0667	0.7	0.7
Roughness (microns)	Minimum		0.2377	1.8150	1.0	1.0
Fy (N)	Minimum		5.1130	35.9933	0.5	0.5
Fx (N)	Minimum		4.6293	27.8933	0.5	0.5

Solutions

Solution	speed (RPM)	feed per tooth (mm/min)	depth of cut (mm)	Temp (celsius) Fit	Roughness (microns) Fit	Fy (N) Fit	Fx (N) Fit	Composite Desirability
1	8000	0.2	0.75	23.9417	0.302333	19.9371	20.3272	0.824570
2	6000	0.2	0.75	23.7417	0.368833	16.2787	21.1587	0.820560
3	8000	0.2	0.5	22.9750	0.641500	18.0629	15.2529	0.805452

Multiple Response Prediction

Variable	Setting
speed (RPM)	8000
feed per tooth (mm/min)	0.2
depth of cut (mm)	0.75

Response	Fit	SE Fit	95% CI	95% PI
Temp (celsius)	23.94	2.18	(18.60, 29.29)	(15.32, 32.56)
Roughness (microns)	0.302	0.359	(-0.576, 1.181)	(-1.115, 1.719)
Fy (N)	19.94	5.87	(5.58, 34.29)	(-3.21, 43.08)
Fx (N)	20.33	5.17	(7.68, 32.98)	(-0.07, 40.72)

a) Roughness

Parameters

Response	Goal	Lower	Target	Upper	Weight	Importance
Temp (celsius)	Minimum		23.2000	34.0667	0.7	0.7
Roughness (microns)	Minimum		0.2377	1.8150	0.5	0.5
Fy (N)	Minimum		5.1130	35.9933	1.0	1.0
Fx (N)	Minimum		4.6293	27.8933	1.0	1.0

Solutions

Solution	speed (RPM)	feed per tooth (mm/min)	depth of cut (mm)	Temp (celsius) Fit	Roughness (microns) Fit	Fy (N) Fit	Fx (N) Fit	Composite Desirability
1	6000	0.1	0.5	26.0750	1.10183	7.9944	8.4541	0.822169
2	8000	0.1	0.5	26.2750	1.03533	11.6528	7.6226	0.799800
3	6000	0.1	0.75	27.0417	0.76267	9.8686	13.5285	0.739826

Multiple Response Prediction

Variable	Setting
speed (RPM)	6000
feed per tooth (mm/min)	0.1
depth of cut (mm)	0.5

Response	Fit	SE Fit	95% CI	95% PI
Temp (celsius)	26.08	2.18	(20.73, 31.42)	(17.46, 34.69)
Roughness (microns)	1.102	0.359	(0.223, 1.981)	(-0.315, 2.519)
Fy (N)	7.99	5.87	(-6.36, 22.35)	(-15.15, 31.14)
Fx (N)	8.45	5.17	(-4.20, 21.10)	(-11.94, 28.85)

b) Force

Figure 4.11 . Output from the response optimizer for a) Roughness and b) Force

Thus, the overall influence of a particular milling condition for minimal temperature, roughness and force with different weights was found. The results from section 4.4.1 suggests that the depth of cut is the most dominant factor for both surface roughness and temperature, while feed rate is the most deterministic factor for cutting force. The reason for the result is because the optimum milling parameters are decided with the input weight factors and the dominant parameters.

CHAPTER 5

CONCLUSIONS AND FUTURE SCOPE

5.1 CONCLUSION

This thesis presents two studies involving two different types of machining processes on cannon bone - drilling and milling.

Experimental study 1 - Vibration assisted drilling of equine cannon bone. The effect of drilling parameters on temperature and thrust force is investigated. Following conclusions are drawn from the results of drilling study:

1) Drill diameter increases in high speed drilling. At 40000 rpm and 60000 rpm, the maximum diameter measured is 3.85mm and 4.85mm at 30mm/min feed speed, and it is 3.45mm and 4.5 mm at 5mm/min respectively. The enlarged diameter is found to be larger than the conventional drilling in the case of vibration assisted drilling. This is because of the pronounced wobbling of toll due to the external vibration.
2) Drilling temperature increases as spindle speed increased from 5000 to 40000rpm. The reason is, increase of tool rotation speed led to an increase in sliding distance between tool and the workpiece for a constant feed speed. There is a decrease in temperature from 40000 rpm to 60000 rpm because of hole enlargement leading to saline irrigation reaching the depths of hole, which resulted in temperature decrease. Same trend is followed in the case of vibration assisted drilling as well. The only

difference is, the magnitude of temperature was less when compared to the conventional drilling because of the Vibration assisted drilling being an intermittent process.

3) Thrust force for vibration assisted drilling is less than the conventional drilling for the most part except at higher spindle speeds. The reason is, in case of enlarged diameter, the tool-bone contact was more in case of vibration assistance because of external vibration, when compared to conventional drilling.
4) In micro-CT images, it can be observed that chunks of materials are attached to the drill hole wall of 60000 rpm samples at 10mm/min and 60000 rpm at 30 mm/min with no vibration because of brittle fracture due to wobbling and less frequent tool contact with the wall. There is more uncut material in 10mm/min when compared to 30mm/min, because of extended brittle fracture with increased time for drilling (slow process).
5) From micro-CT images, it is observed that the diameter is not consistent in vibration assisted drilling, and there is no material attached to the wall. The vibration in z direction along with the wobbling of tool creates larger diameter (elliptical path) may be the reason for this phenomenon. In addition, walls are cleaner due to its frequent contact with the tool.
6) The micro-CT images of lower spindle speeds show cleaner and straighter walls in vibration assisted drilling, while debris remains in the wall in conventional drilling samples.

Therefore, vibration assisted drilling provides less temperature and thrust force at lower spindle speeds when compared to conventional drilling due to intermittent cutting.

Experimental study 2 - Milling of bovine cannon bones. The degree of influence of cutting parameters on temperature, cutting forces and surface roughness created during the milling process was evaluated. Following conclusions are drawn from the milling study:

(1) From Taguchi analysis, depth of cut is observed to be the most influencing parameter on temperature and surface roughness. This is due to the increase in tool contact with the bone which increases the friction, producing more heat. The deformation is also high because of more shear, causing more sticking contact and damaging the milled surface. The feed speed and spindle speed does not influence temperature as much as depth of cut, because a big scale brittle fracture occurs when the front of the cutting edge is parallel to the cutting direction and it collides mechanically to the workpiece in the tool feed per tooth. Temperature does not rise because of brittle fracture [25]. It does not influence surface roughness because of the analytical evaluation by Yeager et al proves otherwise. Also, the larger depth of cut produces larger debris that results in re-deposition on bone matrix causing irregularity in the surface. This phenomenon does not depend on feed rate or spindle speed.

The feed speed is found to be the most influencing parameter on cutting force because the material removal rate increases with increase in feed rate, which results in high milling force. The depth of cut and spindle speed does not affect the cutting force because it does not influence the material removal rate or the impact of tool on the workpiece.

(2) From response optimizer, optimum cutting conditions are found for three different conditions, where each responses having different weights and importance parameters as shown in table 5.1.

Weight values for Responses			Parameters		
Temperature (Celsius)	Surface Roughness (microns)	Milling Forces, Fx, Fy (N)	Spindle speed (rpm)	Feed per tooth (mm/min)	Depth of cut (mm)
1	0.7	0.5	6000	0.2	0.5
0.7	1	0.5	8000	0.2	0.75
0.7	0.5	1	6000	0.1	0.5

Table 5.1 Optimum cutting conditions for various responses

5.2 Recommendations for Future Work

In Vibration Assisted Drilling process, for the measurement of temperature, infrared cameras can be used in the place of thermocouples to reduce the complication of the experiments that can measure temperature within 5% of error. In addition, the vibration frequency and amplitude is kept constant in this study. Further work can examine the effects of different vibrations and frequencies during drilling of equine bone. To observe the effects of higher frequencies, ultrasonic spindle can be used, where the tool is vibrated instead of the workpiece. Histology of drilled bones can be studied for better understanding on the cell's behavior for various conditions.

In milling of bovine cannon bones, for measuring the temperature, infrared cameras can be used instead of thermocouples to reduce the complication. In addition, extending the milling research to various other species and comparing the results will give a better understanding on the consistency of the mechanics of milling and lead to reduced detrimental effects of drilling in bone during orthopedic surgeries.

.

REFERENCES

[1] W. Krause, Orthopaedic cutting procedures, BONEZone, 2 (2003) 4-10.

[2] O.L.A. Harrysson, Y.A. Hosni, J.F. Nayfeh, Custom-designed orthopedic implants evaluated using finite element analysis of patient-specific computed tomography data: femoral-component case study, BMC Musculoskeletal Disorders, 8 (2007) 91-91.

[3] D.P. Haje, J.B. Volpon, Desenvolvimento de parafusos de osso bovino: método de usinagem e estudo metrológico com projetor de perfil, Acta Ortopédica Brasileira, 14 (2006) 87-91.

[4] J.T. Walker, M.C. Rochat, T.A. Snider, M.E. Payton, The relevance of threaded external skeletal fixation pin insertion speed in canine bone with and without predrilling, Veterinary and Comparative Orthopaedics and Traumatology (VCOT), 27 (2014) 249-256.

[5] K. Alam, V.V. Silberschmidt, Analysis of temperature in conventional and ultrasonically-assisted drilling of cortical bone with infrared thermography, Technology and Health Care, 22 (2014) 243-252.

[6] O.M. Pearson, D.E. Lieberman, The aging of Wolff's "law": Ontogeny and responses to mechanical loading in cortical bone, American Journal of Physical Anthropology, 125 (2004) 63-99.

[7] B. Clarke, Normal Bone Anatomy and Physiology, Clinical Journal of the American Society of Nephrology : CJASN, 3 (2008) S131-S139.

[8] V.A. Gibson, S.M. Stover, J.C. Gibeling, S.J. Hazelwood, R.B. Martin, Osteonal effects on elastic modulus and fatigue life in equine bone, Journal of Biomechanics, 39 (2006) 217-22.

[9] E. Shamoto, C. Ma, T. Moriwaki, Ultraprecision ductile cutting of glass by applying ultrasonic elliptical vibration cutting, Precision engineering nanotechnology, 1 (1999) 408-411.

[10] S. Greenberg, D. Gonzalez, E.S. Gurdjian, L. Thomas, Changes in physical properties of bone between the in vivo, freshly dead, and embalmed conditions, in, SAE Technical Paper, 1968.

[11] M. Gustafson, R.B. Martin, V. Gibson, D. Storms, S.M. Stover, J. Gibeling, L. Griffin, Calcium buffering is required to maintain bone stiffness in saline solution, Journal of Biomechanics, 29 (1996) 1191-1194.

[12] S.C. Cowin, Bone mechanics handbook, CRC press, 2001.

[13] R.R. Pelker, G.E. Friedlaender, T.C. Markham, M.M. Panjabi, C.J. Moen, Effects of freezing and freeze-drying on the biomechanical properties of rat bone, Journal of Orthopaedic Research, 1 (1983) 405-411.

[14] J.C. Goh, E.J. Ang, K. Bose, Effect of preservation medium on the mechanical properties of cat bones, Acta Orthopaedica Scandinavica, 60 (1989) 465-467.

[15] F. Linde, H.C.F. Sørensen, The effect of different storage methods on the mechanical properties of trabecular bone, Journal of biomechanics, 26 (1993) 1249-1252.

[16] E.D. Sedlin, A rheologic model for cortical bone: a study of the physical properties of human femoral samples, Acta Orthopaedica Scandinavica, 36 (1965) 1-77.

[17] R.B. Ashman, Ultrasonic determination of the elastic properties of cortical bone: techniques and limitations, in, Tulane University, 1982.

[18] J.K. WEAVER, The microscopic hardness of bone, J Bone Joint Surg Am, 48 (1966) 273-288.

[19] P. Calabrisi, F.C. Smith, The effects of embalming on the compressive strength of a few specimens of compact human bone, Naval Medical Research Institute, National Naval Medical Center, 1951.

[20] J. McElhaney, J. Fogle, E. Byars, G. Weaver, Effect of embalming on the mechanical properties of beef bone, Journal of applied physiology, 19 (1964) 1234-1236.

[21] D. Porta, T. Kress, P. Fuller, J. Snider, Fractures of experimentally traumatized embalmed versus unembalmed cadaver legs, Biomedical sciences instrumentation, 33 (1996) 423-428.

[22] C. Jacobs, M. Pope, J. Berry, F. Hoaglund, A study of the bone machining process—orthogonal cutting, Journal of biomechanics, 7 (1974) 131-136.

[23] K. Wiggins, S. Malkin, Orthogonal machining of bone, Journal of Biomechanical Engineering, 100 (1978) 122-130.

[24] W. Krause, Orthogonal bone cutting: saw design and operating characteristics, Journal of biomechanical engineering, 109 (1987) 263-271.

[25] C. Yeager, A. Nazari, D. Arola, Machining of cortical bone: surface texture, surface integrity and cutting forces, Machining Science and Technology, 12 (2008) 100-118.

[26] K. Alam, A. Mitrofanov, V.V. Silberschmidt, Finite element analysis of forces of plane cutting of cortical bone, Computational Materials Science, 46 (2009) 738-743.

[27] J. Lee, B.A. Gozen, O.B. Ozdoganlar, Modeling and experimentation of bone drilling forces, Journal of biomechanics, 45 (2012) 1076-1083.

[28] M. Arbabtafti, M. Moghaddam, A. Nahvi, M. Mahvash, B. Richardson, B. Shirinzadeh, Physics-based haptic simulation of bone machining, IEEE Transactions on Haptics, 4 (2011) 39-50.

[29] J. Sui, N. Sugita, K. Ishii, K. Harada, M. Mitsuishi, Force analysis of orthogonal cutting of bovine cortical bone, Machining Science and Technology, 17 (2013) 637-649.

[30] K. Denis, G. Van Ham, J. Vander Sloten, R. Van Audekercke, G. Van der Perre, J. De Schutter, J.-P. Kruth, J. Bellemans, G. Fabry, Influence of bone milling parameters on the temperature rise, milling forces and surface flatness in view of robot-assisted total knee arthroplasty, in: International congress series, Elsevier, 2001, pp. 300-306.

[31] P. Bast, M. Engelhardt, W. Lauer, K. Schmieder, V. Rohde, K. Radermacher, Identification of milling parameters for manual cutting of bicortical bone structures, Computer Aided Surgery, 8 (2003) 257-263.

[32] P.A. Federspil, U.W. Geisthoff, D. Henrich, P.K. Plinkert, Development of the First Force-Controlled Robot for Otoneurosurgery, The Laryngoscope, 113 (2003) 465-471.

[33] H. Thompson, Effect of drilling into bone, Journal of oral surgery, 16 (1958) 22.

[34] R. Vaughn, F. Peyton, The influence of rotational speed on temperature rise during cavity preparation, Journal of dental research, 30 (1951) 737-744.

[35] L.S. Matthews, C. Green, S. Goldstein, The thermal effects of skeletal fixation-pin insertion in bone, J Bone Joint Surg Am, 66 (1984) 1077-1083.

[36] G. Augustin, S. Davila, K. Mihoci, T. Udiljak, D.S. Vedrina, A. Antabak, Thermal osteonecrosis and bone drilling parameters revisited, Archives of Orthopaedic and Trauma Surgery, 128 (2008) 71-77.

[37] D.L. Brisman, The effect of speed, pressure, and time on bone temperature during the drilling of implant sites, International Journal of Oral & Maxillofacial Implants, 11 (1996).

[38] M. Hillery, I. Shuaib, Temperature effects in the drilling of human and bovine bone, Journal of Materials Processing Technology, 92 (1999) 302-308.

[39] K.N. Bachus, M.T. Rondina, D.T. Hutchinson, The effects of drilling force on cortical temperatures and their duration: an in vitro study, Medical engineering & physics, 22 (2000) 685-691.

[40] O. Nam, W. Yu, M.Y. Choi, H.M. Kyung, Monitoring of bone temperature during osseous preparation for orthodontic micro-screw implants: Effect of motor speed and ressure, in: Key Engineering Materials, Trans Tech Publ, 2006, pp. 1044-1047.

[41] M. Sharawy, C.E. Misch, N. Weller, S. Tehemar, Heat generation during implant drilling: the significance of motor speed, Journal of Oral and Maxillofacial Surgery, 60 (2002) 1160-1169.

[42] L.S. Matthews, C. Hirsch, Temperatures measured in human cortical bone when drilling, J Bone Joint Surg Am, 54 (1972) 297-308.

[43] P.-I. Branemark, Osseointegration and its experimental background, The Journal of prosthetic dentistry, 50 (1983) 399-410.

[44] S. Itay, H. Tsur, Thermal osteonecrosis complicating Steinmann pin insertion in plastic surgery, Plastic and reconstructive surgery, 72 (1983) 557-561.

[45] T. Udiljak, D. Ciglar, S. Skoric, Investigation into bone drilling and thermal bone necrosis, Advances in Production Engineering & Management, 2 (2007) 103-112.

[46] V. Kalidindi, Optimization of drill design and coolant systems during dental implant surgery, (2004).

[47] G. Augustin, S. Davila, T. Udilljak, T. Staroveski, D. Brezak, S. Babic, Temperature changes during cortical bone drilling with a newly designed step drill and an internally cooled drill, International orthopaedics, 36 (2012) 1449-1456.

[48] C. Jacob, J. Berry, M. Pope, F. Hoaglund, A study of the bone machining process—drilling, Journal of Biomechanics, 9 (1976) 343IN3345-3344IN5349.

[49] S.R. Davidson, D.F. James, Measurement of thermal conductivity of bovine cortical bone, Medical Engineering & Physics, 22 (2000) 741-747.

[50] Y.-K. Tu, W.-H. Lu, L.-W. Chen, C.-H. Chiang, Y.-C. Chen, H.-H. Tsai, Thermal contact simulation of drill bit and bone during drilling, in: Bioinformatics and

Biomedical Engineering (iCBBE), 2010 4th International Conference on, IEEE, 2010, pp. 1-4.

[51] J. Lee, Y. Rabin, O.B. Ozdoganlar, A new thermal model for bone drilling with applications to orthopaedic surgery, Medical engineering & physics, 33 (2011) 1234-1244.

[52] R.K. Pandey, S.S. Panda, Drilling of bone: A comprehensive review, Journal of Clinical Orthopaedics and Trauma, 4 (2013) 15-30.

[53] R. Wootton, J. Reeve, N. Veall, The clinical measurement of skeletal blood flow, Clinical Science, 50 (1976) 261-268.

[54] M. Xiao, K. Sato, S. Karube, T. Soutome, The effect of tool nose radius in ultrasonic vibration cutting of hard metal, International Journal of Machine Tools and Manufacture, 43 (2003) 1375-1382.

[55] M. Zhou, Y.T. Eow, B.K.A. Ngoi, E.N. Lim, Vibration-Assisted Precision Machining of Steel with PCD Tools, Materials and Manufacturing Processes, 18 (2003) 825-834.

[56] H. Weber, J. Herberger, R. Pilz, Turning of Machinable Glass Ceramics with an Ultrasonically Vibrated Tool, CIRP Annals - Manufacturing Technology, 33 (1984) 85-87.

[57] C. Ma, E. Shamoto, T. Moriwaki, Y. Zhang, L. Wang, Suppression of burrs in turning with ultrasonic elliptical vibration cutting, International Journal of Machine Tools and Manufacture, 45 (2005) 1295-1300.

[58] E. Shamoto, T. Moriwaki, Study on Elliptical Vibration Cutting, CIRP Annals - Manufacturing Technology, 43 (1994) 35-38.

[59] N. Suzuki, A. Nakamura, E. Shamoto, K. Harada, M. Matsuo, M. Osada, Ultraprecision micromachining of hardened steel by applying ultrasonic elliptical

vibration cutting, in: Micromechatronics and Human Science, 2003. MHS 2003. Proceedings of 2003 International Symposium on, 2003, pp. 221-226.

[60] C. Nath, M. Rahman, K.S. Neo, Machinability study of tungsten carbide using PCD tools under ultrasonic elliptical vibration cutting, International Journal of Machine Tools and Manufacture, 49 (2009) 1089-1095.

[61] A. Mitrofanov, N. Ahmed, V. Babitsky, V. Silberschmidt, Effect of lubrication and cutting parameters on ultrasonically assisted turning of Inconel 718, Journal of materials processing technology, 162 (2005) 649-654.

[62] R. Skelton, Effect of ultrasonic vibration on the turning process, International Journal of Machine Tool Design and Research, 9 (1969) 363-374.

[63] A.V. Mitrofanov, V.I. Babitsky, V.V. Silberschmidt, Finite element simulations of ultrasonically assisted turning, Computational Materials Science, 28 (2003) 645-653.

[64] Y.L. Zhang, Z.M. Zhou, Z.H. Zia, Diamond turning of titanium alloy by applying ultrasonic vibration, TRANSACTIONS OF NONFERROUS METALS SOCIETY OF CHINA, 15 (2005) 279-282.

[65] C. Nath, M. Rahman, Effect of machining parameters in ultrasonic vibration cutting, International Journal of Machine Tools and Manufacture, 48 (2008) 965-974.

[66] M. Xiao, S. Karube, T. Soutome, K. Sato, Analysis of chatter suppression in vibration cutting, International Journal of Machine Tools and Manufacture, 42 (2002) 1677-1685.

[67] M. Xiao, Q.M. Wang, K. Sato, S. Karube, T. Soutome, H. Xu, The effect of tool geometry on regenerative instability in ultrasonic vibration cutting, International Journal of Machine Tools and Manufacture, 46 (2006) 492-499.

[68] G.-L. Chern, Y.-C. Chang, Using two-dimensional vibration cutting for micro-milling, International Journal of Machine Tools and Manufacture, 46 (2006) 659-666.

[69] H. Ding, R. Ibrahim, K. Cheng, S.-J. Chen, Experimental study on machinability improvement of hardened tool steel using two dimensional vibration-assisted micro-end-milling, International Journal of Machine Tools and Manufacture, 50 (2010) 1115-1118.

[70] X.-H. Shen, J.-H. Zhang, H. Li, J.-J. Wang, X.-C. Wang, Ultrasonic vibration-assisted milling of aluminum alloy, Int J Adv Manuf Technol, 63 (2012) 41-49.

[71] M.M.A. Zarchi, M.R. Razfar, A. Abdullah, Investigation of the effect of cutting speed and vibration amplitude on cutting forces in ultrasonic-assisted milling, PROCEEDINGS OF THE INSTITUTION OF MECHANICAL ENGINEERS PART B-JOURNAL OF ENGINEERING MANUFACTURE, 226 (2012) 1185-1191.

[72] M.M. Abootorabi Zarchi, M.R. Razfar, A. Abdullah, Influence of ultrasonic vibrations on side milling of AISI 420 stainless steel, Int J Adv Manuf Technol, 66 (2013) 83-89.

[73] C.Y. Hsu, C.K. Huang, C.Y. Wu, Milling of MAR-M247 nickel-based superalloy with high temperature and ultrasonic aiding, Int J Adv Manuf Technol, 34 (2007) 857-866.

[74] K.-M. Li, S.-L. Wang, Effect of tool wear in ultrasonic vibration-assisted micro-milling, Proceedings of the Institution of Mechanical Engineers, Part B: Journal of Engineering Manufacture, 228 (2014) 847-855.

[75] X.-H. Shen, J. Zhang, D. Xing, Y. Zhao, A study of surface roughness variation in ultrasonic vibration-assisted milling, Int J Adv Manuf Technol, 58 (2012) 553-561.

[76] G. Novajra, N.G. Boetti, J. Lousteau, S. Fiorilli, D. Milanese, C. Vitale-Brovarone, Phosphate glass fibre scaffolds: Tailoring of the properties and enhancement of the bioactivity through mesoporous glass particles, Materials Science and Engineering: C, 67 (2016) 570-580.

[77] W.Y. Lee, N. Li, S. Lin, B. Wang, H.Y. Lan, G. Li, miRNA-29b improves bone healing in mouse fracture model, Molecular and cellular endocrinology, 430 (2016) 97-107.

[78] A. Larrue, A. Rattner, Z.-A. Peter, C. Olivier, N. Laroche, L. Vico, F. Peyrin, Synchrotron Radiation Micro-CT at the Micrometer Scale for the Analysis of the Three-Dimensional Morphology of Microcracks in Human Trabecular Bone, PLoS ONE, 6 (2011) e21297.

[79] K. Kadirgama, M. Noor, M. Rahman, K. Abou-El-Hossein, B. Mohammad, H. Habeeb, Effect of milling parameters on frictions when milling hastelloy C-22HS: A FEM and statistical method, Trends in Applied Sciences Research, 4 (2009) 216-228.

[80] N. Sugita, S.i. Warisawa, M. Mitsuishi, A cutting temperature study of bone machining for orthopaedic robotic surgery, in: Proceedings of the 20th Annual Meeting of the American Society for Precision Engineering, 2005, pp. 142-145.

VITA

ARJUN DHAMODHARAN

Candidate for the Degree of

Master of Science

Thesis: ANALYSIS OF BONE CUTTING MECHANICS IN ORTHOPEDIC SURGERY

Major Field: Mechanical and Aerospace Engineering

Biographical:

Education:

Completed the requirements for the Master of Science in Mechanical and Aerospace Engineering at Oklahoma State University, Stillwater, Oklahoma in July, 2016.

Completed the requirements for the Bachelor of Technology in Mechanical Engineering at Amrita School of Engineering, Coimbatore, India in 2012.

Experience:

Worked as a Graduate Research Assistant in Precision Manufacturing Processes Laboratory in Oklahoma State University from May 2014 to July 2016.

Worked as Graduate Teaching Assistant in the School of Mechanical and Aerospace Engineering at Oklahoma State University from August 2014 to May 2016.

Professional Memberships:

Member of International SAE from August 2010 to Dec 2013.

Member of ASME from May 2014.